

# Correlations of Structure with Binding Ability Involving Nine Hemicarcerand Hosts and Twenty-Four Guests<sup>1</sup>

Roger C. Helgeson, Carolyn B. Knobler, and Donald J. Cram\*

Contribution from the Department of Chemistry and Biochemistry, University of California at Los Angeles, Los Angeles, California 90095

Received September 26, 1996. Revised Manuscript Received February 4, 1997<sup>⊗</sup>

**Abstract:** Hemicarcerands **1–9**, composed by coupling through four O(CH<sub>2</sub>)<sub>4</sub>O or four 1,3-(OCH<sub>2</sub>)<sub>2</sub>C<sub>6</sub>H<sub>4</sub> bridging units in different pair combinations of three tetrol bowls (varying spanners, O(CH<sub>2</sub>)<sub>n</sub>O, *n* = 1, 2, or 3), have been examined for their abilities to incarcerate a variety of organic guest compounds of widely differing structures. When the conformationally flexible tetrol bowl (spanners = O(CH<sub>2</sub>)<sub>3</sub>O) was coupled lip-to-lip to either of two rigid bowl units (spanners = OCH<sub>2</sub>O or O(CH<sub>2</sub>)<sub>2</sub>O), the rigid units tended to impose their shapes on the mobile units in the resulting hosts (<sup>1</sup>H NMR spectral and crystal structure evidence). Complexes were formed by heating to high temperatures host dissolved in a large excess of guest. High structural recognition in complexation was observed for the 1,3-(OCH<sub>2</sub>)<sub>2</sub>C<sub>6</sub>H<sub>4</sub>-bridged hosts to favor binding of 1,2-disubstituted as compared to 1,3- and 1,4-disubstituted benzenes as guests. Three new crystal structures of hemicarceplexes identical except for their spanner lengths are compared, and a fourth new structure allows comparison of identical hosts with different guests. Decomplexation rates are compared in some cases. Interesting new kinds of restricted rotations of guests with respect to hosts were observed. Three examples of trace impurities in guests being scavenged by the host were encountered.

The syntheses and characterizations of hemicarcerands **1–9** and their cavitand precursors **10–12** (Chart 1) are described elsewhere.<sup>2,3</sup> Here we report the results of a survey of the binding properties of hosts **1–9** toward selected organic guests composed of between six and 13 non-hydrogen atoms. The sizes and shapes of guest candidates must be complementary enough to the host's portals and interiors so that *constrictive* and *intrinsic binding*<sup>4</sup> taken together allow hemicarceplexes to be formed at high temperatures, yet the complexes must be stable enough at ambient temperature to be isolable and manipulable.

Hosts **1–6** all contain four 1,3-(OCH<sub>2</sub>)<sub>2</sub>C<sub>6</sub>H<sub>4</sub> groups that link the northern and southern hemispheres to one another (bridging groups), but differ in the lengths of the four O(CH<sub>2</sub>)<sub>n</sub>O moieties (spanning groups) that maintain the general bowl-like shape of each hemisphere. Notice that **1** contains only OCH<sub>2</sub>O, **2** only O(CH<sub>2</sub>)<sub>2</sub>O, and **3** only O(CH<sub>2</sub>)<sub>3</sub>O spanners in each host, making the northern and southern hemispheres identical. In contrast, **4** combines O(CH<sub>2</sub>)<sub>2</sub>O (northern) with OCH<sub>2</sub>O (southern); **5**, O(CH<sub>2</sub>)<sub>3</sub>O with OCH<sub>2</sub>O; and **6**, O(CH<sub>2</sub>)<sub>3</sub>O with O(CH<sub>2</sub>)<sub>2</sub>O as spanning groups. To invoke images of **1–6**, we refer to **1** as **MM** (methylene–methylene), **2** as **EE** (ethylene–ethylene), **3** as **PP** (propylene–propylene), **4** as **EM**, **5** as **PM** and **6** as **PE**. The R groups in **7–10**, **12–14**, and similarly positioned groups in other hosts are called feet, and in Corey–Pauling–Koltun (CPK) models have little effect on the cavities and portals of the hosts. In **1–7** and **9–12** these groups are all C<sub>5</sub>H<sub>11</sub>. In **13** and **14**, they are CH<sub>3</sub> and in most other studied hosts including **8**, R = CH<sub>2</sub>CH<sub>2</sub>Ph.<sup>5</sup> Notice that **7–9** contain the shorter

O(CH<sub>2</sub>)<sub>4</sub>O bridges, and **7** and **8** possess OCH<sub>2</sub>O, and **9**, O(CH<sub>2</sub>)<sub>2</sub>O spanners.<sup>2</sup>

Crystal structures of **13**<sup>2</sup> (a close relative of **10**) and of **8**<sup>3</sup> each possess an approximate C<sub>4</sub> axis. Crystal structures of **11** and of **9**,<sup>2</sup> a close relative of **2**, both exhibit approximate C<sub>2</sub> symmetry that deviates from C<sub>4</sub> by about 9% in **11** but by only 4% in **9**.<sup>2</sup> A crystal structure of **14**, a model for **12**, possesses mirror (C<sub>s</sub>) symmetry, but deviates from C<sub>4</sub> by 37%.<sup>2</sup>

Molecular models (CPK)<sup>6</sup> of **3**, **5** and **6** that contain **P** units can be assembled only if the conformations of the O(CH<sub>2</sub>)<sub>3</sub>O spanners provide their hemispheres with an approach to C<sub>4</sub> symmetry. The two simplest conformations of **P** units in **PP**, **PE**, and **PM** in models that possess C<sub>4</sub> axes and minimize C–O dipole–dipole energies are (1) that in which the four *bridges* are *outward* (**bo**) and the *spanners* are *upward* (**su** as drawn in **12**); (2) that in which the four *bridges* are *inward* (**bi**) and the *spanners* are *outward* (**so**). The **P** units in the **bo-su** conformation shorten polar axes, lengthen equatorial axes, and shrink the portals in hemicarcerands, while **P** units in the **bi-so** conformation lengthen polar axes, shorten equatorial axes, and enlarge portals in hemicarcerands. For example, host **PP** (**3**) in the **bo-su** conformation has essentially no portals, but has very large portals in the **bi-so** conformation. In CPK models, the **M** and **E** units have relatively little conformational mobility.<sup>2</sup> Models of hemicarcerands **1–6** in those conformations which maximize their portal sizes assume the order **PP** > **PM** > **MM** > **PE** > **EM** > **EE**. However, the host's portal adaptability to guest shape for complexation–decomplexation provides the order **PP** > **PM** > **PE** > **MM** > **EM** > **EE**. The hosts in those conformations that appear to maximize their inner volume have the order, **PP** > **PE** > **EE** > **PM** > **EM** > **MM**. The order of shell-closure yields leading to these six hemicarcerands is **MM** > **EE** > **PE** > **EM** > **PP** > **PM**.<sup>2</sup>

## Results

**Complexation.** Table 1 indicates which host@guest combinations form isolable complexes from hosts **1–9** and **24**

(6) Koltun, W. L. *Biopolymers*, **1965**, *3*, 665–679.

<sup>⊗</sup> Abstract published in *Advance ACS Abstracts*, March 15, 1997.

(1) Host–Guest Complexation, 68.

(2) Helgeson, R. C.; Paek, K.; Knobler, C. B.; Maverick, E. F.; Cram, D. J. *J. Am. Chem. Soc.* **1996**, *118*, 5590–5604.

(3) Robbins, T. A.; Knobler, C. B.; Bellew, D. R.; Cram, D. J. *J. Am. Chem. Soc.* **1994**, *116*, 111–122.

(4) Cram, D. J.; Blanda, M. T.; Paek, K.; Knobler, C. B. *J. Am. Chem. Soc.* **1992**, *114*, 7765–7773.

(5) Cram, D. J.; Cram, J. M. *Container Molecules and Their Guests. Monographs in Supramolecular Chemistry*; Stoddart, J. F., Ed.; The Royal Society of Chemistry: Thomas Graham House, Science Park, Cambridge, U.K. 1994; pp 131–216.

Chart 1

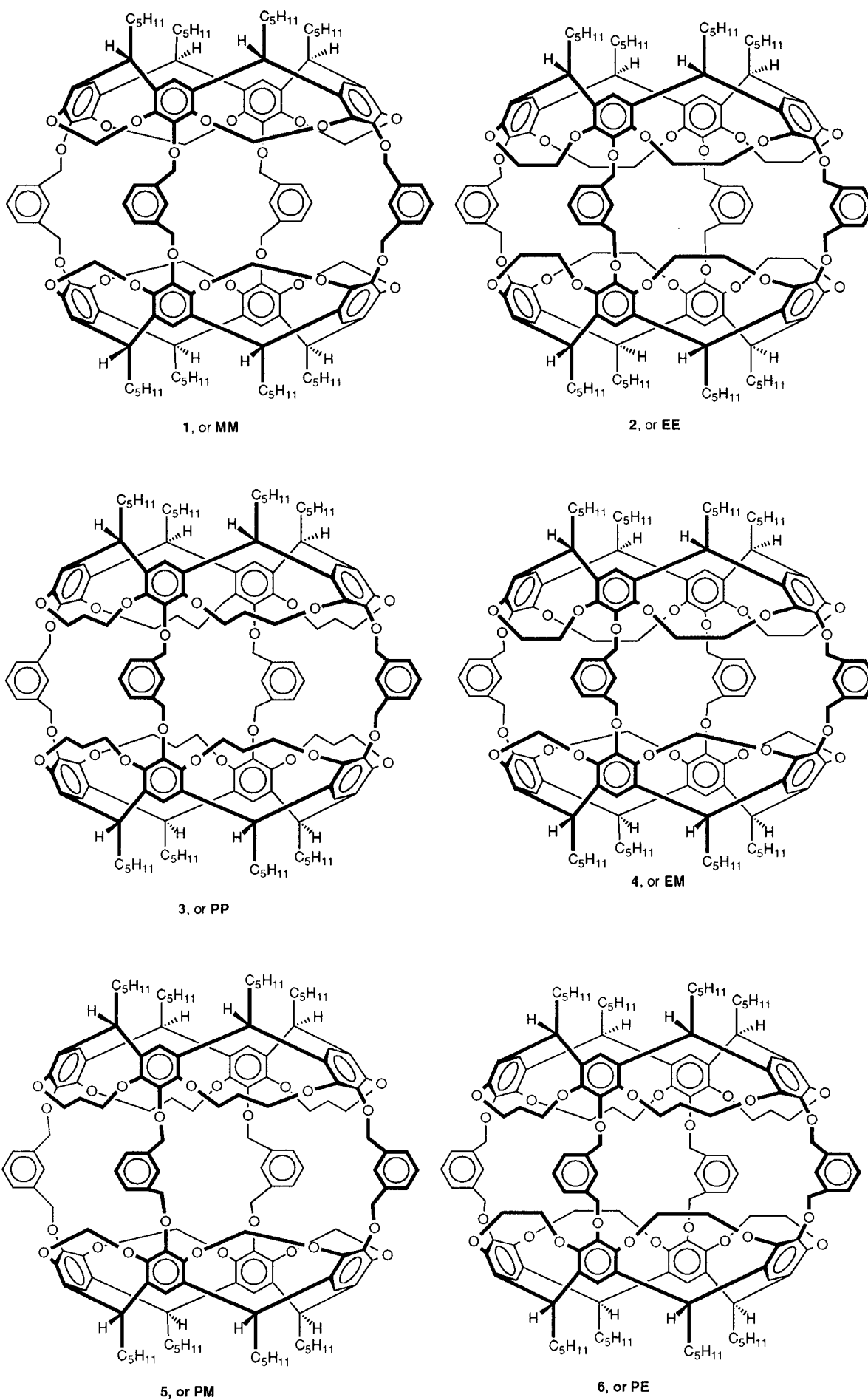
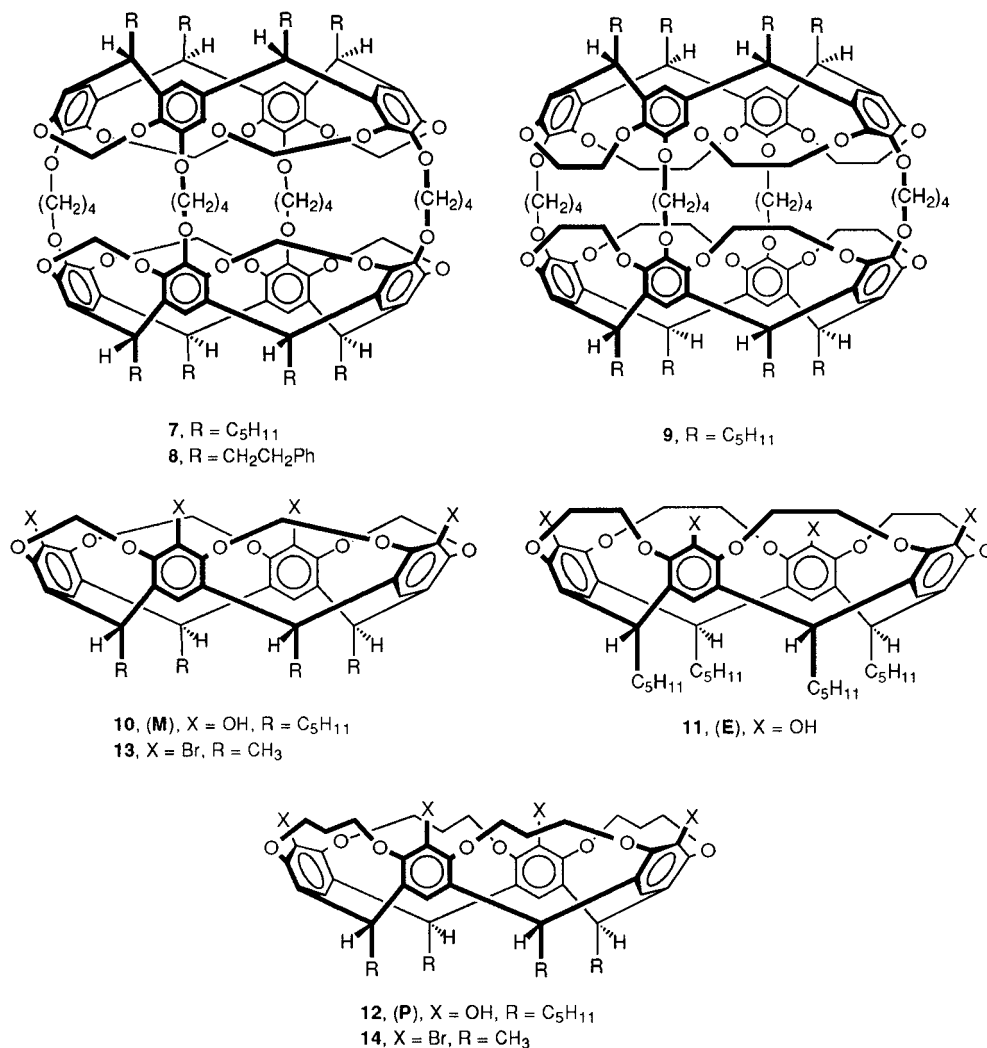


Chart I (continued)



different guests. Each complex is assigned a number. Of the 40 complexes obtained, 35 were formed by heating homogeneous liquid phases composed of free host, at least 1000-fold excess of guest, and when needed, Ph<sub>2</sub>O as solvent. Model examinations show that Ph<sub>2</sub>O is too large and unadaptable to enter any of the hosts except **MM** (**1**), **PM** (**5**), and **PP** (**6**). The cooled reaction mixtures were flooded with MeOH, the precipitated complexes were washed, dried, and chromatographed (silica gel plates—CH<sub>2</sub>Cl<sub>2</sub>—hexane for most of the complexes). Table 1 provides the conditions for the thermally induced complexation and shows how each complex was characterized. The other five complexes were obtained by shell closures (**15** or **7**⊙Me<sub>2</sub>SO, **16** or **8**⊙Me<sub>2</sub>SO,<sup>3</sup> **17** or **9**⊙Me<sub>2</sub>SO<sup>2</sup>, **22** or **MM**⊙Ph<sub>2</sub>O and **53** or **PM**⊙1,2,3-(MeO)<sub>3</sub>C<sub>6</sub>H<sub>3</sub><sup>2</sup>). The complex **15** (**7**⊙Me<sub>2</sub>SO) is new, but prepared by standard procedures.<sup>2,3</sup> The <sup>1</sup>H NMR spectral changes of host and guest in CDCl<sub>3</sub> solution at 25 °C before and after complexation ( $\Delta\delta = \delta_{\text{free}} - \delta_{\text{complexed}}$ ) are collated with their structures in Table 2.

All complexes gave FAB-MS in which the *m/e* values coincided with (host⊙guest)<sup>+</sup> as the dominant signal, or at least as a very substantial signal. An understandable exception is **32** (**EE**⊙PhCH(Me)CH<sub>2</sub>Me). The <sup>1</sup>H NMR spectra of all complexes showed them to be one-to-one. Those complexes obtained in a pure state (32 out of 37 new complexes) when submitted to elemental analysis gave results within 0.40% of theory.

**Scavenging of Trace Impurities.** In three attempts to form complexes in which guests served as the solvent, low concentra-

tions of isomeric impurities were incarcerated faster than the bulk solvent: (1) When Aldrich "99% Me<sub>3</sub>CPh" (in our hands 2% PhCH(Me)CH<sub>2</sub>Me by GC-MS) was used as a medium for complexing **EE** (72 h at 150 °C), a 2:1 ratio of **33** (**EE**⊙Me<sub>3</sub>CPh) to **32** (**EE**⊙PhCH(Me)CH<sub>2</sub>Me) was isolated, indicating that PhCH(Me)CH<sub>2</sub>Me was incarcerated ~25 times faster than Me<sub>3</sub>CPh. At 25 °C in CDCl<sub>3</sub>, **32** (**EE**⊙PhCH(Me)CH<sub>2</sub>Me) decomplexed much faster than **33** (**EE**⊙Me<sub>3</sub>CPh), which was stable indefinitely. (2) When 3-ClC<sub>6</sub>H<sub>4</sub>COMe was used as solvent in an attempt to complex **EE** (96 h, 150 °C), a mixture of **EE**⊙3-ClC<sub>6</sub>H<sub>4</sub>COMe and empty **EE** (ratio 44:55, respectively) was formed. In an attempt to form **EE**⊙4-ClC<sub>6</sub>H<sub>4</sub>COMe (96 h, 150 °C), only **41** (**EE**⊙2-ClC<sub>6</sub>H<sub>4</sub>COMe) and free **EE** (ratio 2:1, respectively) were obtained. Thus the relative rates of complexation of **EE** by the three isomeric guests were 1,2-isomer ≫ 1,3-isomer ≫ ≫ 1,4-isomer. Only **41** (**EE**⊙2-ClC<sub>6</sub>H<sub>4</sub>COMe) was obtained pure and was characterized. (3) When 1,3,5-Me<sub>3</sub>C<sub>6</sub>H<sub>3</sub> containing **EE** was heated to 150 °C for 3 days, only **31** (**EE**⊙1,2,4-Me<sub>3</sub>C<sub>6</sub>H<sub>3</sub>) was obtained. Thus 1,2,4-Me<sub>3</sub>C<sub>6</sub>H<sub>3</sub> ≫ 1,3,5-Me<sub>3</sub>C<sub>6</sub>H<sub>3</sub> in rate of incarceration. The scavenging of low levels of impurities of structural isomers points to high levels exercised by the host for structural recognition in complexation.

**Crystal Structures of 37 or EE⊙4-MeC<sub>6</sub>H<sub>4</sub>OMe, 52 or PE⊙4-MeC<sub>6</sub>H<sub>4</sub>OMe, 50 or PE⊙1,2-(MeO)<sub>2</sub>C<sub>6</sub>H<sub>4</sub>, and 55 or EM⊙4-MeC<sub>6</sub>H<sub>4</sub>OMe.** All four of the new crystal structures reported here belong to the triclinic space group P1, and all four require a disorder model.

**Table 1.** Thermal Conditions for Complexation, Isolation Procedures, and Characterization of Complexes<sup>a</sup>

complex no.	complexing partners		medium	<i>T</i> (°C)	<i>t</i> (days)	isolation procedure <sup>b</sup>	yield (%)	FAB MS (M <sup>+</sup> ) (obs (%))		C + H anal. <sup>c</sup>
	host	guest						<i>m/e</i> complex	<i>m/e</i> host	
15	7	Me <sub>2</sub> SO	Me <sub>2</sub> SO <sup>d</sup>	70	3	<i>d</i>	18 <sup>d</sup>	2057 (100)	1978 (70)	yes
16	8	Me <sub>2</sub> SO	Me <sub>2</sub> SO <sup>d</sup>	70	5	<i>d</i>	18 <sup>d</sup>	2329 (100)	2251 (35)	yes
17	9	Me <sub>2</sub> SO	Me <sub>2</sub> SO <sup>d</sup>	74	2	<i>d</i>	9 <sup>d</sup>	2167 (100)		yes
18	MM	CBBr <sub>2</sub> HCBBr <sub>2</sub> H	guest	105	1.5	A	65	2520 (40)	2170 (100)	yes
19	MM	Me <sub>3</sub> CCOMe	guest + Ph <sub>2</sub> O <sup>e</sup>	100	5	B	~30 <sup>a</sup>	2270 (30) <sup>a</sup>	2170 (100)	no <sup>a</sup>
20	MM	Me <sub>3</sub> C(OH)C(OH)Me <sub>2</sub>	guest + Ph <sub>2</sub> O <sup>e</sup>	160	2	A	40	2290 (25)	2170 (100)	yes
21	MM	Me <sub>3</sub> CPh	guest	160	3	B	62	2305 (100)	2170 (75)	yes
22	MM	Ph <sub>2</sub> O	guest + NMP <sup>f,g</sup>	65	3	<i>g</i>	10	2343 (100)	2170 (5)	yes
23	MM	1,2,3-(MeO) <sub>3</sub> C <sub>6</sub> H <sub>3</sub>	guest	160	2	A	74	2339 (100)	2170 (15)	yes
24	MM	1,2,3-(MeO) <sub>3</sub> -5-HOC <sub>6</sub> H <sub>2</sub>	guest + Ph <sub>2</sub> O <sup>e</sup>	150	1.5	A	40	2354 (100)	2170 (5)	yes
25	EM	Me <sub>3</sub> CPh	guest	160	3	B	65	2360 (100)	2226 (60)	yes
26	EM	1,2,3-(MeO) <sub>3</sub> C <sub>6</sub> H <sub>3</sub>	guest	160	2	A	70	2396 (100)	2226 (25)	yes
27	EE	MePh	guest	110	1.5	B	76	2376 (85)	2282 (100)	yes
28	EE	1,2-Me <sub>2</sub> C <sub>6</sub> H <sub>4</sub>	guest	130	2	B	60	2389 (100)	2282 (55)	yes
29	EE	1,3-Me <sub>2</sub> C <sub>6</sub> H <sub>4</sub>	guest	130	1.5	B	75	2389 (95)	2282 (100)	yes
30	EE	1,4-Me <sub>2</sub> C <sub>6</sub> H <sub>4</sub>	guest	130	2	B	80	2389 (35)	2282 (100)	yes
31	EE	1,2,4-Me <sub>3</sub> C <sub>6</sub> H <sub>3</sub>	guest	160	2	B	81	2404 (100)	2282 (60)	yes
32	EE	PhCH(Me)CH <sub>2</sub> Me	guest	160	3	B	70	2404 <sup>h</sup> (35)	2282 (100)	yes <sup>i</sup>
33	EE	Me <sub>3</sub> CPh	guest	160	11	B	~40 <sup>a</sup>	2417 (70) <sup>a</sup>	2282 (100)	no <sup>a</sup>
34	EE	1,2-(MeO) <sub>2</sub> C <sub>6</sub> H <sub>4</sub>	guest	130	2	B	60	2421 (100)	2282 (50)	yes
35	EE	1,4-(MeO) <sub>2</sub> C <sub>6</sub> H <sub>4</sub>	guest + Ph <sub>2</sub> O <sup>e</sup>	160	3	B	30	2421 (30)	2282 (100)	no
36	EE	1,2,3-(MeO) <sub>3</sub> C <sub>6</sub> H <sub>3</sub>	guest	160	3	A	62	2451 (100)	2282 (35)	yes
37	EE	4-MeC <sub>6</sub> H <sub>4</sub> OMe	guest	150	1	B	64	2404 (20)	2282 (100)	yes
38	EE	coumarin	guest + Ph <sub>2</sub> O <sup>e</sup>	185	4	C	47	2430 (30)	2282 (100)	yes
39	EE	PhCOMe	guest	160	2	B	78	2403 (50)	2282 (100)	yes
40	EE	2-MeC <sub>6</sub> H <sub>4</sub> COMe	guest	160	3	B	55	2417 (100)	2282 (70)	yes
41	EE	2-ClC <sub>6</sub> H <sub>4</sub> COMe	guest	150	4	B	70	2437 (100)	2282 (75)	yes
42	EE	2-BrC <sub>6</sub> H <sub>4</sub> COMe	guest	150	2	B	~35 <sup>a</sup>	2481 (40)	2282 (100)	no <sup>a</sup>
43	EE	2-MeOC <sub>6</sub> H <sub>4</sub> COMe	guest	160	2	A	68	2434 (100) <sup>a</sup>	2282 (100)	yes
44	EE	2-ClC <sub>6</sub> H <sub>4</sub> CO <sub>2</sub> Me	guest	150	3	B	46	2454 (85)	2282 (100)	yes
45	PE	Me <sub>3</sub> CPh	guest	160	2	B	50	2473 (65)	2338 (100)	yes
46	PE	coumarin	guest + Ph <sub>2</sub> O <sup>e</sup>	160	4	B	50	2487 (60)	2338 (100)	yes
47	PE	PhCOMe	guest	160	1	B	75	2458 (75)	2338 (100)	yes
48	PE	2-MeC <sub>6</sub> H <sub>4</sub> COMe	guest	160	3	B	65	2473 (100)	2338 (65)	yes
49	PE	2-MeOC <sub>6</sub> H <sub>4</sub> COMe	guest	160	2	A	70	2489 (65)	2338 (100)	yes
50	PE	1,2-(MeO) <sub>2</sub> C <sub>6</sub> H <sub>4</sub>	guest	160	2	B	55	2476 (90)	2338 (100)	yes
51	PE	1,2,3-(MeO) <sub>3</sub> C <sub>6</sub> H <sub>3</sub>	guest	160	2	A	50	2507 (85)	2338 (100)	yes
52	PE	4-MeC <sub>6</sub> H <sub>4</sub> OMe	guest	150	1	B	70	2459 (45)	2338 (100)	yes
53	PM	1,2,3-(MeO) <sub>3</sub> C <sub>6</sub> H <sub>3</sub>	<i>d</i>	60	2	<i>d</i>	1.8 <sup>d</sup>	2449 (100)	2281 (80)	yes
54	PP	Me <sub>3</sub> CPh	guest	160	3	B	~35 <sup>a</sup>	2529 (60) <sup>a</sup>	2394 (100)	no <sup>a</sup>

<sup>a</sup> All pure complexes gave expected <sup>1</sup>H NMR spectra, detailed in Table 2. Inseparable but purified mixtures of host and complex, analyzed by <sup>1</sup>H NMR spectra, were obtained in the ratios as follows: **1/19** (MM/MM⊙Me<sub>3</sub>CCOMe) = 1; **2/33** (EE/EE⊙Me<sub>3</sub>CPh) = 0.9; **2/42** (EE/EE⊙2-BrC<sub>6</sub>H<sub>4</sub>COMe) = 1; **3/54** (PP/PP⊙Me<sub>3</sub>CPh) = 1. Yields were corrected with these ratios. Elemental analyses were not performed but FAB MS were obtained from these mixtures. <sup>b</sup> See Experimental Section. <sup>c</sup> Carbon and hydrogen elemental analyses are within 0.40% of theory. <sup>d</sup> Complex formed by shell closure only (refs 2 and 3). <sup>e</sup> Ratio 1:1 (w/w). <sup>f</sup> NMP is *N*-methylpyrrolidinone. <sup>g</sup> Shell-closure reaction with 19:1 (v/v) NMP-Ph<sub>2</sub>O (see Experimental Section). <sup>h</sup> (M minus Me). <sup>i</sup> This complex contains 3H<sub>2</sub>O.

The host in the crystal structure (298 K) of **37** (EE⊙4-MeC<sub>6</sub>H<sub>4</sub>OMe) lies on a center of symmetry. There are four interstitial 4-MeC<sub>6</sub>H<sub>4</sub>OMe molecules, in addition to the incarcerated 4-MeC<sub>6</sub>H<sub>4</sub>OMe guest. The four bridge oxygen atoms of each cavitated moiety (bowl) are coplanar within 0.00 Å and form an approximate square, with angles of 86.9, 87.9, 90.5, and 94.8°. The guest 4-MeC<sub>6</sub>H<sub>4</sub>OMe must be modeled with disorder because it is non-like-ended and it lies on a center of symmetry. In the refined model, all the non-hydrogen guest atoms are coplanar.

Neither the host nor the guest of the hemicarceplex in the crystal structure (175 K) of **52** (PE⊙4-MeC<sub>6</sub>H<sub>4</sub>OMe) can be centrosymmetric, but their departures from being centrosymmetric are small enough for the complex to fall on a crystallographic center of symmetry. The required disorder in the host is confined to the regions of the spanners, which embrace the disordered Me and MeO groups of the guest, whose non-hydrogen atoms are coplanar. The four bridge oxygen atoms of each bowl are within 0.02 Å of being coplanar and form a near square whose angles are 88.7, 88.9, 90.0, and 92.3°. There is one interstitial 4-MeC<sub>6</sub>H<sub>4</sub>OMe molecule in the unit cell.

In the crystal structure (175 K) of **50** (PE⊙1,2-(MeO)<sub>2</sub>C<sub>6</sub>H<sub>4</sub>)

the disorder is similar to that in **52** (PE⊙4-MeC<sub>6</sub>H<sub>4</sub>OMe). The two cavitated moieties in each complex have different spanners, but every other part of the host seems to conform to the center of symmetry so that the host disorder is only apparent in the spanner region. One molecule of 1,2-(MeO)<sub>2</sub>C<sub>6</sub>H<sub>4</sub> is located in the host cavity of its complex. Since this guest is not centrosymmetric it is also disordered. The bridge oxygen atoms from one cavitated moiety are coplanar within 0.04 Å and form a near square, with angles 86.3, 90.4, 90.5, and 92.8°. Six additional 1,2-(MeO)<sub>2</sub>C<sub>6</sub>H<sub>4</sub> molecules crystallize with the hemicarceplex.

In the crystal structure (298 K) of **55** (EM⊙4-MeC<sub>6</sub>H<sub>4</sub>OMe), the disorder is similar to that in the two PE complexes. There are four interstitial 4-MeC<sub>6</sub>H<sub>4</sub>OMe molecules per molecule of complex. The bridge oxygen atoms from one cavitated moiety are coplanar within 0.00 Å and form a near square, with angles 87.9, 88.7, 90.8, and 92.6°.

Table 3 contains side stereoviews of these four crystal structures, and top stereoviews including only the oxygen squares (connected with straight lines), bridges and guest. Notice in the top stereoviews that in all four structures the guest's aryl plane is diagonally arranged with respect to the

two near squares, which are neither rotated nor displaced with respect to one another. A view from the bottom of **52** ( $\text{PE}\odot\text{4-MeC}_6\text{H}_4\text{OMe}$ ) minus feet is portrayed, as well as a similar view minus one bowl and the feet. Table 3 also includes for comparisons stereoviews of **17** ( $\text{9}\odot\text{Me}_2\text{SO}$ ).<sup>2</sup> All eight spanners of **9** are  $\text{OCH}_2\text{CH}_2\text{O}$ , and the host in the crystal structure possesses a center of symmetry. The top view of the oxygen "squares", guest, and bridges shows that the two sets of bridge oxygens are more nearly diamond shaped than square. Note that the bridge carbons of **55** ( $\text{EM}\odot\text{4-MeC}_6\text{H}_4\text{OMe}$ ), **37** ( $\text{EE}\odot\text{4-MeC}_6\text{H}_4\text{OMe}$ ), **52** ( $\text{PE}\odot\text{4-MeC}_6\text{H}_4\text{OMe}$ ), **50** ( $\text{PE}\odot\text{1,2-(MeO)}_2\text{C}_6\text{H}_4$ ), and **17** ( $\text{9}\odot\text{Me}_2\text{SO}$ ) all lie outside the volume described by the eight bridging oxygens of the hosts. Table 4 provides parameter values taken from the crystal structures of **55**, **37**, **52**, **50**, **17**,<sup>2</sup> **11**,<sup>2</sup> and **14**<sup>2</sup> which bear on the questions of the effects of bowl incorporation into hemicarcerands, and of the effects of different guests, on bowl structure in hemicarcerands.

## Discussion

**Formation of Hemicarceplexes Stable to Isolation and Purification.** The complexes of **1–6** listed in Table 5 were formed by the thermal equilibration and precipitation method except for **53** ( $\text{PM}\odot\text{1,2,3-(MeO)}_3\text{C}_6\text{H}_3$ ), which was formed during shell closure. Complex **22** ( $\text{MM}\odot\text{Ph}_2\text{O}$ ) was formed by both methods. Those compounds selected for trial as guests were chosen on the basis of our ability to force CPK models (new bonds) of guest into models of the host, frequently with considerable difficulty and repeated trials, but without breaking bonds. The more complete testing of **PM** and **PP** as hosts was prevented by their very limited availability.

The isolable complexes listed in Table 5 contain guests composed of 6–13 atoms other than hydrogen. The simplest of these ( $\text{Br}_2\text{CHCHBr}_2$ ) contains the four large bromine atoms and two trisubstituted carbons. The next smallest is  $\text{C}_6\text{H}_5\text{CH}_3$  (seven rigidly disposed carbons), followed by  $\text{Me}_2\text{C(OH)C(OH)Me}_2$  (six carbons, two quaternary, plus two oxygens), and the xylenes (eight coplanar carbons). Most of the other guests are di- or trisubstituted benzenes. The two guests that formed the most complexes (five each) were  $\text{Me}_3\text{CC}_6\text{H}_5$  (contains a quaternary carbon and a phenyl) and  $\text{1,2,3-(MeO)}_3\text{C}_6\text{H}_3$  (is rigidified by the 1,2,3-trisubstituted pattern). In general, the guests that formed the most complexes were those which for steric or electronic reasons extend substantially into all three dimensions. Interestingly, 1,2-disubstituted benzenes complexed and decomplexed hosts more easily than their 1,3- and 1,4-disubstituted isomers. In CPK models, the guest  $\text{1,4-(MeO)}_2\text{C}_6\text{H}_4$  of **35** ( $\text{EE}\odot\text{1,4-(MeO)}_2\text{C}_6\text{H}_4$ ), positioned so that the long guest axis is coincident with the polar axis of the host, fully uses the available length of this dimension of the cavity. Attempts to form the following complexes in isolable form failed, although <sup>1</sup>H NMR spectral evidence for their fleeting presence in  $\text{CDCl}_3$  was observed:  $\text{EE}\odot\text{Me(CH}_2)_4\text{Me}$ ,  $\text{MM}\odot\text{MePh}$ ,  $\text{MM}\odot\text{4-MeC}_6\text{H}_4\text{OMe}$ ,  $\text{MM}\odot\text{MeCOPh}$ ,  $\text{MM}\odot\text{1,2-(MeO)}_2\text{C}_6\text{H}_4$ ,  $\text{MM}\odot\text{1,4-(MeO)}_2\text{C}_6\text{H}_4$ ,  $\text{EM}\odot\text{MeCOPh}$  and  $\text{PE}\odot\text{6-methylcoumarin}$ . Complexes particularly slow to form were **41** ( $\text{EE}\odot\text{2-ClC}_6\text{H}_4\text{COMe}$ ), **42** ( $\text{EE}\odot\text{2-BrC}_6\text{H}_4\text{COMe}$ ), **33** ( $\text{EE}\odot\text{Me}_3\text{CPh}$ ), and **54** ( $\text{PP}\odot\text{Me}_3\text{CPh}$ ). Model examination of  $\text{1,3,5-Me}_3\text{C}_6\text{H}_3$  and **EE** suggested no complex should form, and none was observed (3 d, 150 °C).

Failure to obtain particular hemicarceplexes of hosts **1–9** can be due to any of three reasons: (1) The guests are too large to pass through the portals of the host at elevated temperature because the sizes or shapes of the portals and guests are too noncomplementary. The kinetic barrier to complexation is too large to be overcome by thermal means. (2) The free host and

guest are thermodynamically more stable than is their complex, to an extent great enough to overcome the mass law driving force for complexation provided by the > 1000-fold concentration excess of guest over host in the binding experiments. For example, a guest may be too large or ill-shaped to fit into the host's cavity, which possesses limited adaptability. Alternatively, if the host and guest are complementary but the entropy of binding is large and negative and the complexation activation free energy is high enough to require too high a temperature to reach equilibration,  $T\Delta S$  values at that temperature may strongly favor free host and guest.<sup>4</sup> (3) The guest is small enough to enter and depart the interior of the host with a low enough activation energy at ambient temperature so that mass law-driven exchange of guest with solvent occurs during isolation of the complex. Methanol was chosen as precipitant for the complexes because if it ever entered the host, it was lost during the chromatographic purification of the complex, since it was never detected in <sup>1</sup>H NMR or mass spectra of the products.

**Crystal Structure Comparisons.** Comparisons of the crystal structure parameters (Table 4) of **55** ( $\text{EM}\odot\text{4-MeC}_6\text{H}_4\text{OMe}$ ), **37** ( $\text{EE}\odot\text{4-MeC}_6\text{H}_4\text{OMe}$ ), **52** ( $\text{PE}\odot\text{4-MeC}_6\text{H}_4\text{OMe}$ ), **50** ( $\text{PE}\odot\text{1,2-(MeO)}_2\text{C}_6\text{H}_4$ ), **17** ( $\text{9}\odot\text{Me}_2\text{SO}$ ), tetrol bowl **11** (**E**), and tetrabromide bowl **14** (**P**) provide interesting conclusions about the effects of guest shapes, bridging, and spanner groups on bowl dimensions and shapes. Most obviously different is the diamond-shaped arrangement of the much less coplanar oxygens in **17** ( $\text{9}\odot\text{Me}_2\text{SO}$ , four  $\text{O(CH}_2)_4\text{O}$  bridges) and in bowl **11**, which become near-square and coplanar in **55** ( $\text{EM}\odot\text{4-MeC}_6\text{H}_4\text{OMe}$ ), **37** ( $\text{EE}\odot\text{4-MeC}_6\text{H}_4\text{OMe}$ ), **52** ( $\text{PE}\odot\text{4-MeC}_6\text{H}_4\text{OMe}$ ), and **50** ( $\text{PE}\odot\text{1,2-(MeO)}_2\text{C}_6\text{H}_4$ ). The  $\text{C}\cdots\text{C}$  diagonal length differences in the carbon **b** plane in diagram **56** (Table 4) provide a measure of the constraint the bridges put on the bowls pushing them toward the square arrangement. These differences in  $\text{C}\cdots\text{C}$  diagonal lengths (Å) decrease as follows: bowl **14**, 5.59; bowl **11**, 1.47; **17** ( $\text{9}\odot\text{Me}_2\text{SO}$ ), 0.75; **50** ( $\text{PE}\odot\text{1,2-(MeO)}_2\text{C}_6\text{H}_4$ ), 0.31; **52** ( $\text{PE}\odot\text{4-MeC}_6\text{H}_4\text{OMe}$ ), 0.10; **37** ( $\text{EE}\odot\text{4-MeC}_6\text{H}_4\text{OMe}$ ), 0.06; **55** ( $\text{EM}\odot\text{4-MeC}_6\text{H}_4\text{OMe}$ ), 0.03 Å. The out-of-plane C atom distances (Å) for plane **b** (diagram **56**) also provide a measure of how much the bridges impose shapes on the bowls (see Table 4). Both criteria indicate  $\text{1,3-(OCH}_2)_2\text{C}_6\text{H}_4$  bridges >  $\text{O(CH}_2)_4\text{O}$  bridges > no bridges in pushing the **E** and **P** bowls toward a  $\text{C}_4$  arrangement in the hemicarcerand hosts. This order reflects the coplanarity imposed by the *m*-xylyl unit on five of the seven atoms of the bridge in **EM**, **EE**, and **PE** hosts, and the greater conformational freedom of the  $\text{O(CH}_2)_4\text{O}$  (six atom) bridges.

The four-carbon atom planes **c** and **d** (diagram **56**, Table 4) are much less sensitive to the bridges and spanners than are planes **a** and **b**. For example, the  $(\text{C}\cdots\text{C})_{\text{av}}$  distances (Å) for the diagonals of plane **c** range between a high of 5.26 for **14** to a low of 5.10 for **11**, the distances for the five complexes lying between these two values. The C out-of-plane **c** distances are all small, varying from  $\pm 0.07$  to  $\pm 0.01$  Å. The  $(\text{C}\cdots\text{C})_{\text{av}}$  distances (Å) for the diagonals of plane **d** (the carbons of the feet attached directly to the bowl) also vary only slightly with changes in the bridges and spanners, between values of 7.38 and 7.20 Å. The C out-of-plane **d** distances all vary only between  $\pm 0.00$  and  $\pm 0.03$  Å for the seven systems. Thus the structures of the polar regions of both the cavitands and hemicarcerands are relatively insensitive to changes in spanners and bridges.

The crystal structures of **52** ( $\text{PE}\odot\text{4-MeC}_6\text{H}_4\text{OMe}$ ) and **50** ( $\text{PE}\odot\text{1,2-(MeO)}_2\text{C}_6\text{H}_4$ ) at 175 K are particularly interesting because the hosts are the same but the guests are different. Furthermore, each host includes two sets of bowls that differ in their spanners, one being **P** or  $\text{OCH}_2\text{CH}_2\text{CH}_2\text{O}$  and the other

**Table 2.** Chemical Shift Changes ( $\Delta\delta$ ) in 500 MHz  $^1\text{H}$  NMR Spectra in  $\text{CDCl}_3$  at 25  $^\circ\text{C}$  that Accompany Complexation of Hosts and Guests

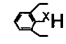
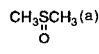
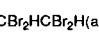
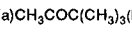
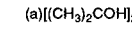
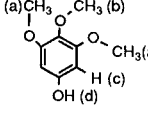
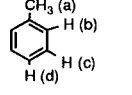
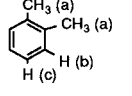
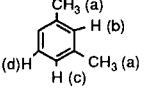
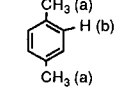
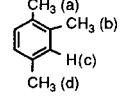
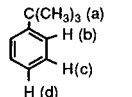

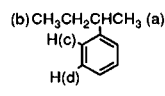
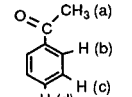
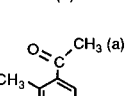
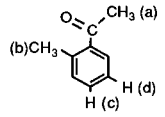
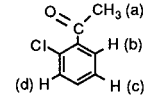
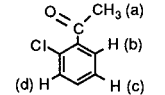
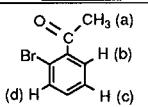
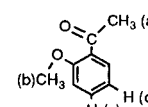
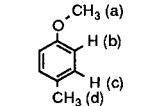
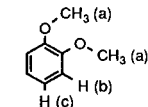
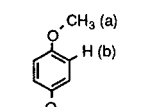
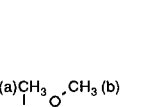
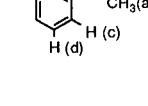
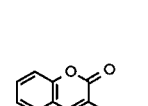
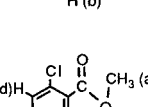
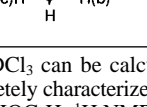
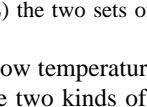
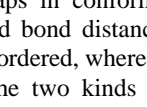
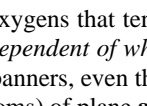
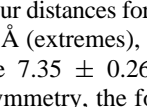

compl. numb.	carceplexing partners		complexed guest $\delta$ (ppm)				complexed guest $\delta\Delta$ (ppm) <sup>a</sup>				host  of bridge (ppm)		
	host	guest structure	<sup>a</sup> H	<sup>b</sup> H	<sup>c</sup> H	<sup>d</sup> H	<sup>a</sup> H	<sup>b</sup> H	<sup>c</sup> H	<sup>d</sup> H	free $\delta$	complex $\delta$	$\Delta\delta$
15	7 <sup>b</sup>		-0.46				2.92						
16	8 <sup>c</sup>		-0.49				2.95						
17	9		-0.80				3.26						
18	MM		5.07				0.98			7.46	7.57	-0.11	
19	MM		-0.26	-0.06			2.41	1.21		7.46	7.67	-0.21	
20	MM		-0.27				2.51			7.46	7.60	-0.14	
24	MM <sup>d</sup>		-0.23	2.85	4.53		4.08	0.88	1.54	7.62 <sup>d</sup>	7.21	+0.41	
27	EE		-0.74	7.20	7.20	7.20	3.12	1.68	1.78	3.53	7.88	7.87	+0.01
28	EE		0.27	e	e		1.99				7.88	7.85	+0.03
29	EE		-0.65	e	4.66	6.63	2.93		2.29	0.48	7.88	7.85	+0.03
30	EE		-1.24	5.54			3.54	1.44			7.88	7.82	+0.06
31	EE		-1.08	e	4.68	-1.31	3.30		2.27	3.59	7.88	7.78	+0.10
21	MM		0.00	6.32	5.54	3.58	1.32	1.09	1.84	3.59	7.46	7.25	+0.21
25	EM		-0.26	5.90	5.04	e	1.58	1.51	2.34		7.60	7.57	+0.03
33	EE		-0.27	5.48	5.33	3.68	1.59	1.93	2.05	3.49	7.88	7.77	+0.11
45	PE		-0.64	5.78	5.45	3.25	1.96	1.63	1.93	3.92	7.95	7.94	+0.01
54	PP		-0.64	5.64	4.21	e	1.96	1.77	3.17		8.02	7.86	+0.16
32	EE		-0.87	0.81	6.17	5.55	2.11	0.00	1.00	1.73	7.88	7.93	-0.05
39	EE		-0.87	6.22	5.52	4.25	3.47	1.75	1.94	3.29	7.88	7.93	-0.05
47	PE		-0.79	6.07	5.53	4.22	3.39	1.90	1.93	3.32	7.95	8.05	-0.10
40	EE		-0.74	e	e	6.45	3.32			0.80	7.88	7.78	+0.10
48	PE		-0.62	e	5.93		3.20		1.45		7.95	7.95	0.00
41	EE		-0.69	5.98	6.33	4.42	3.34	1.61	1.02	2.98	7.88	7.84	+0.04

Table 2 (Continued)

compl. numb.	carceplexing partners	complexed guest $\delta$ (ppm)	complexed guest $\delta\Delta$ (ppm) <sup>a</sup>				host of bridge (ppm) of free complex					
			<sup>a</sup> H	<sup>b</sup> H	<sup>c</sup> H	<sup>d</sup> H	$\delta$	$\delta$	$\Delta\delta$			
42	EE 	-0.67	5.91	6.51	4.51	3.31	1.71	0.80	2.95	7.88	7.80	+0.08
43	EE 	-0.81	e	6.30	3.42	3.42		1.16	0.58	7.88	7.85	+0.03
49	PE 	-0.55	e	e	e	3.16				7.95	7.98	-0.03
37	EE 	0.42	5.39	5.51	-1.34	3.36	1.41	1.58	3.63	7.88	7.78	+0.10
52	PE 	0.42	5.30	5.42	-0.99	3.36	1.50	1.67	3.28	7.95	7.91	+0.04
34	EE 	1.80	4.73	4.92		2.08	2.17	1.98		7.88	7.84	+0.04
50	PE 	1.84	4.76	4.93		2.04	2.14	1.97		7.95	7.98	-0.03
35	EE 	0.37	5.44			3.40	1.42			7.88	7.82	+0.06
23	MM 	-0.11	2.85	5.18	6.43	3.96	1.01	1.40	0.56	7.46	7.30	+0.16
26	EM 	-0.44 <sup>f</sup> 0.32 <sup>f</sup>	2.92	4.92	6.46	4.29 <sup>f</sup> 3.53 <sup>f</sup>	0.94	1.66	0.53	7.60	7.40	+0.20
36	EE 	0.34	2.92	4.77	6.52	3.51	0.94	1.81	0.47	7.88	7.69	+0.19
53	PM 	-0.21	3.01	5.22	6.45	4.06	0.85	1.36	0.54	g	7.35	
51	PE 	0.76	2.90	4.62	e	3.09	0.96	1.96		7.95	7.80	+0.15
38	EE 	2.92	4.28	e	e	3.50	3.42			7.88	7.98	-0.10
46	PE 	3.05	4.48	e	e	3.37	3.22			7.95	8.09	-0.14
44	EE 	0.34	6.36	e	e	3.56	1.46			7.88	7.77	+0.11

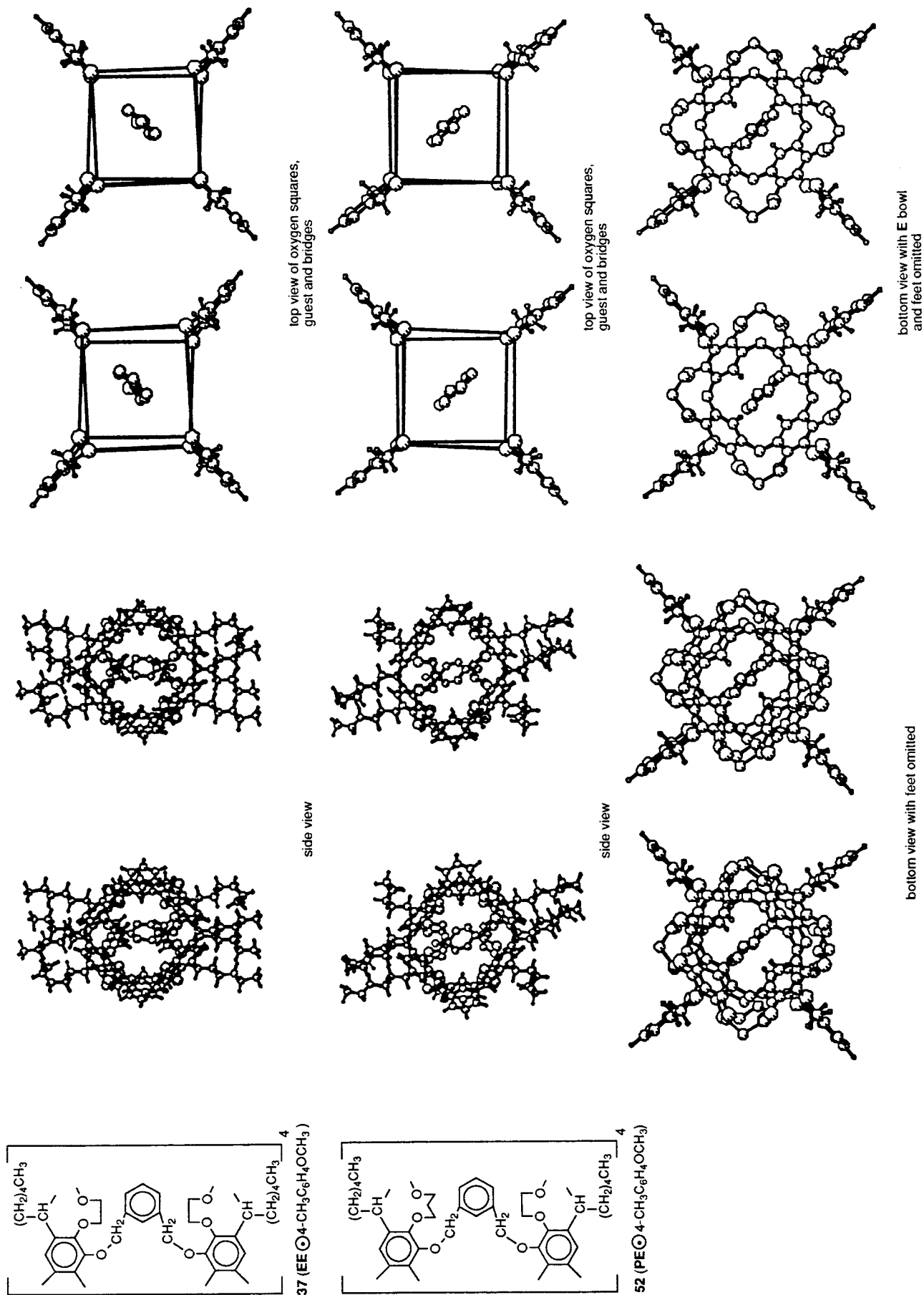
<sup>a</sup> Free guest  $\delta$  values in  $\text{CDCl}_3$  can be calculated from the equation:  $\delta_{\text{free}} = \Delta\delta + \delta_{\text{complexed}}$ . **MM** $\odot$ Ph<sub>2</sub>O <sup>1</sup>H NMR data are given in the text.

<sup>b</sup> Unpublished results on completely characterized complex prepared by standard procedures (ref 3), T. A. Robbins and D. J. Cram. <sup>c</sup> Feet =  $\text{CH}_2\text{CH}_2\text{Ph}$ , ref 3. <sup>d</sup> **MM** $\odot$ 1,2,3-(MeO)<sub>3</sub>-5-HOC<sub>6</sub>H<sub>2</sub> <sup>1</sup>H NMR spectrum was taken in  $\text{CDCl}_2\text{CDCl}_2$ . <sup>e</sup> Signal obscured by other peaks. <sup>f</sup> For **EM** $\odot$ 1,2,3-(MeO)<sub>3</sub>C<sub>6</sub>H<sub>3</sub> (not for **MM**, **EE**, **PM**, or **EE**) the two sets of <sup>a</sup>H have different  $\delta$ . <sup>g</sup> Free **PM** was not prepared.

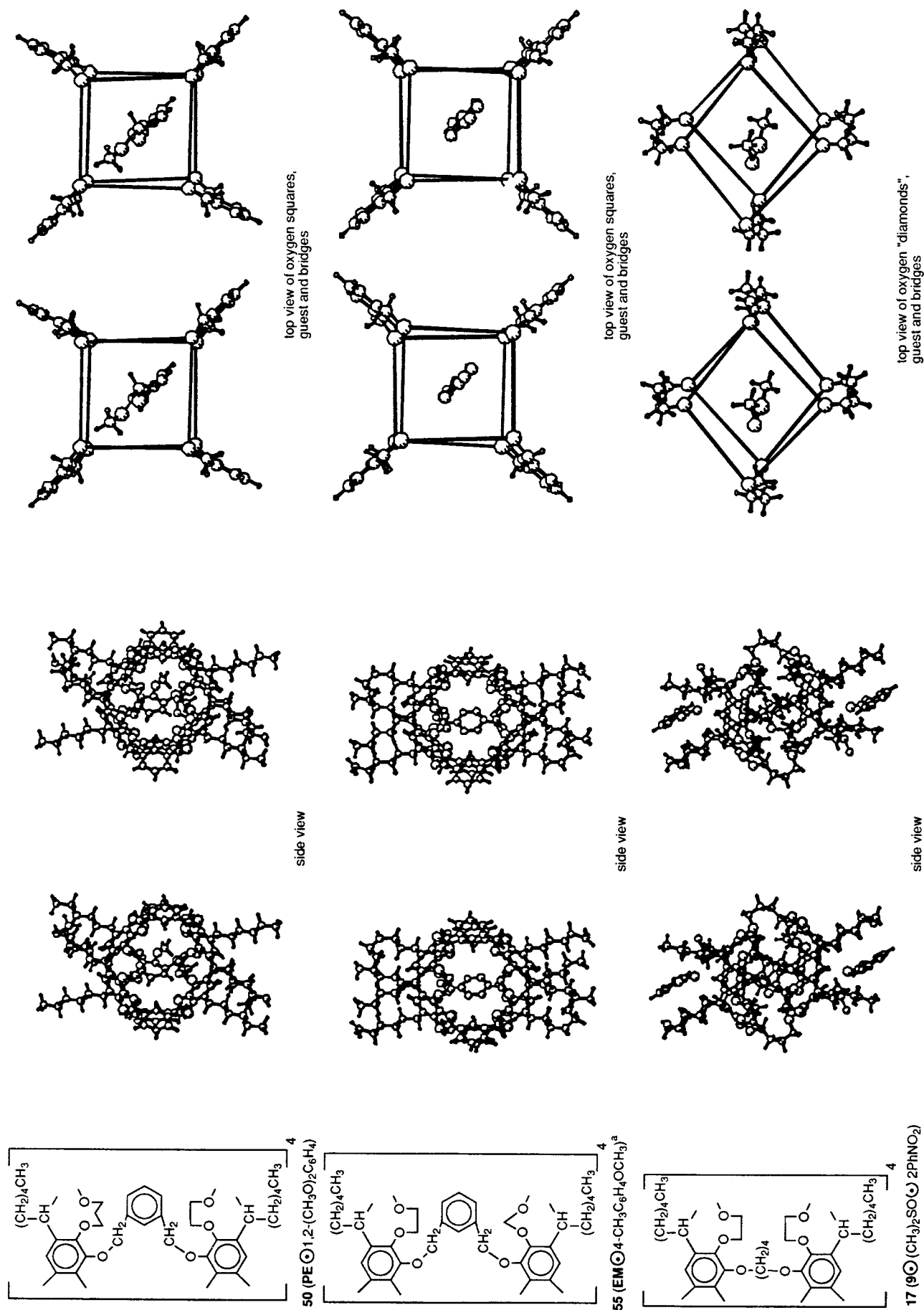
**E**, or  $\text{OCH}_2\text{CH}_2\text{O}$ . At the low temperature in both complexes, all five carbon atoms of the two kinds of spanners are visible in the electron density maps in conformations that provide reasonable bond angles and bond distances. In **50**, some of the spanner oxygens are disordered, whereas in **52** the positions of the oxygen atoms of the two kinds of spanners are not discernibly different. Thus the remarkable feature of the structure of **52** is that the oxygens that terminate each spanner are in positions that are independent of whether they terminate  $\text{CH}_2\text{CH}_2\text{CH}_2$  or  $\text{CH}_2\text{CH}_2$  spanners, even though the four  $\text{O}\cdots\text{O}$  edge distances (bridge O atoms) of plane **a** are all different (see **56** of Table 4). The latter four distances for **52** (**PE** $\odot$ 4-MeC<sub>6</sub>H<sub>4</sub>-OMe) average  $7.32 \pm 0.15$  Å (extremes), and for **50** (**PE** $\odot$ 1,2-(MeO)<sub>2</sub>C<sub>6</sub>H<sub>4</sub>) they average  $7.35 \pm 0.26$  Å (extremes). As required by the center of symmetry, the four distances in each

complex are the same for the two kinds of bowls, and all the other parameters given in Table 4 for **52** (**PE** $\odot$ 4-MeC<sub>6</sub>H<sub>4</sub>OMe) and for **50** (**PE** $\odot$ 1,2-(MeO)<sub>2</sub>C<sub>6</sub>H<sub>4</sub>) are identical and independent of their locations in the **P** or **E** parts of the hosts. Thus only one column of values needs to be listed for each hemicarceplex. Furthermore, in looking along the central polar axis of each host (bottom views in Table 3), all host atoms in the near hemisphere except the carbons of the spanners approximately eclipse the host atoms in the far hemisphere, even though the hosts do not have a crystallographic  $C_4$  axis. Even the diagonally related 1,3-(OCH<sub>2</sub>)<sub>2</sub>C<sub>6</sub>H<sub>4</sub> bridges are nearly coplanar. Finally, the hosts' **P** and **E** bowls are not further disordered in the lattice. In the structures of **52** (**PE** $\odot$ 4-MeC<sub>6</sub>H<sub>4</sub>OMe) and **50** (**PE** $\odot$ 1,2-(MeO)<sub>2</sub>C<sub>6</sub>H<sub>4</sub>), all spanners are distinguishable at 175 K, although not at 298 K in the former structure.

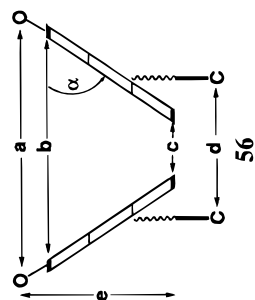
Table 3. Stereoviews of Crystal Structures







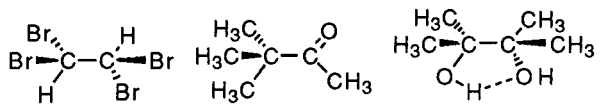
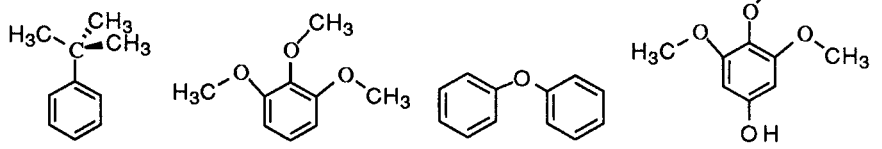
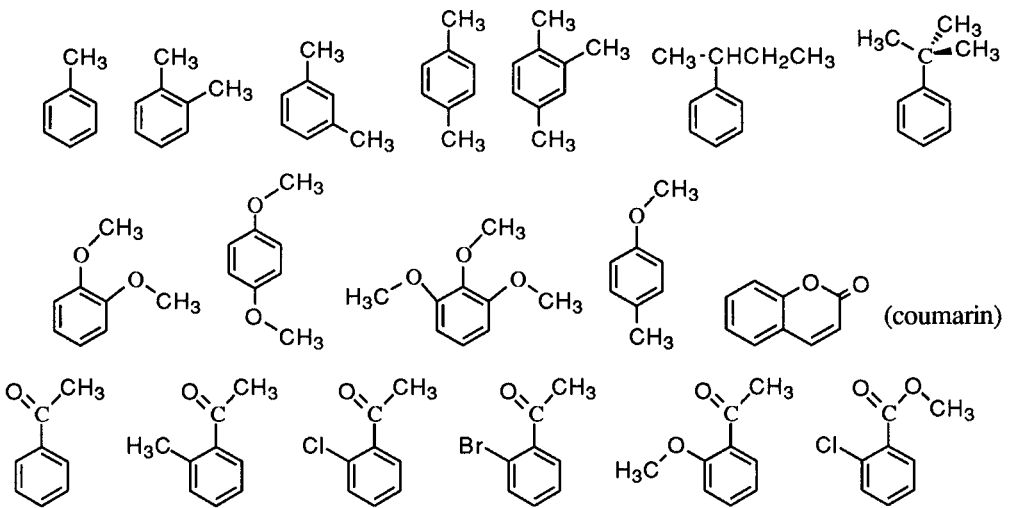
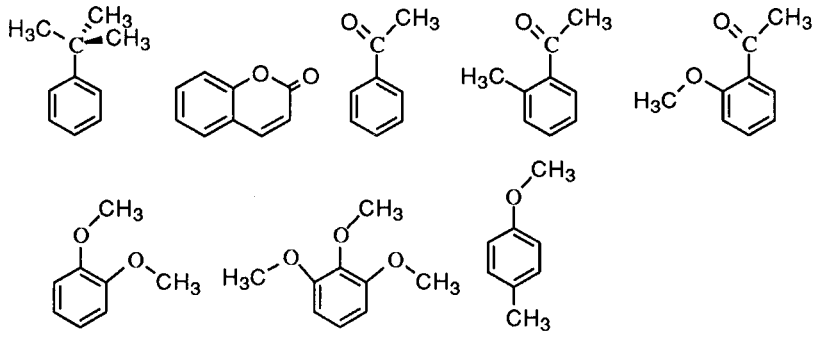
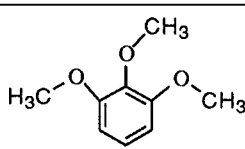
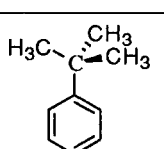
<sup>a</sup> This complex was omitted from Tables 1 and 2 since it was uncharacterizable except by crystal structure determination.

**Table 4.** Distances in Crystal Structures Relevant to Effects on Bowl and Bridge Structures of their Being Incorporated into Hemicerand

distance (Å) <sup>a</sup>	carceplexes				cavitand bowls		
	<b>55</b> or <b>EM</b> ⊙4-MeC <sub>6</sub> H <sub>4</sub> OMe	<b>37</b> or <b>EE</b> ⊙4-MeC <sub>6</sub> H <sub>4</sub> OMe	<b>52</b> or <b>PE</b> ⊙4-MeC <sub>6</sub> H <sub>4</sub> OMe	<b>50</b> or <b>PE</b> ⊙1,2-(MeO) <sub>2</sub> C <sub>6</sub> H <sub>4</sub>	<b>17</b> or <b>9</b> ⊙Me <sub>2</sub> SO <sup>b</sup>	<b>11</b> <sup>b</sup>	<b>14</b> <sup>b</sup>
O...O edge, plane <b>a</b>	6.95, 6.72, 6.88, 6.55	6.68, 7.23, 6.92, 7.33	7.17, 7.38, 7.25, 7.47	7.09, 7.45, 7.33, 7.52	6.92, 7.47, 7.37, 7.08	7.25, 7.44, 7.42, 7.54	
(O...O) <sub>av</sub> edge, plane <b>a</b>	6.78	7.04	7.32	7.35	7.21	7.41	
O...O diagonals, plane <b>a</b>	9.56, 9.60	9.89, 10.01	10.29, 10.40	10.24, 10.53	9.46, 10.84	9.24, 11.46	
(O...O) <sub>av</sub> diagonals plane <b>a</b>	9.58	9.95	10.34	10.38	10.15	10.35	
O...O diagonal, difference	0.04	0.12	0.11	0.29	1.38	2.22	
C...C diagonals, plane <b>b</b>	8.17, 8.20	8.47, 8.41	8.71, 8.61	8.55, 8.86	8.22, 8.97	7.87, 9.34	10.39, 4.80
(C...C) <sub>av</sub> diagonals plane <b>b</b>	8.18	8.44	8.66	8.70	8.60	8.60	7.60
C...C diagonal, difference	0.03	0.06	0.10	0.31	0.75	1.47	5.59
C out-of-plane <b>b</b> <sup>c</sup>	± 0.00	± 0.01	± 0.01	± 0.03	± 0.10	± 0.26	± 1.12
C...C diagonals, plane <b>c</b>	5.25, 5.21	5.21, 5.20	5.23, 5.14	5.11, 5.20	5.13, 5.10	5.13, 5.08	5.48, 5.05
(C...C) <sub>av</sub> diagonals, plane <b>c</b>	5.23	5.20	5.18	5.16	5.12	5.10	5.26
C out-of-plane <b>c</b> <sup>c</sup>	± 0.02	± 0.02	± 0.01	± 0.01	± 0.04	± 0.03	± 0.07
C...C diagonals, plane <b>d</b>	7.20, 7.22	7.27, 7.23	7.19, 7.23	7.20, 7.21	7.21, 7.21	7.17, 7.24	7.38, 7.38
(C...C) <sub>av</sub> diagonals plane <b>d</b>	7.21	7.25	7.21	7.20	7.21	7.20	7.38
C out-of-plane <b>d</b> <sup>c</sup>	± 0.02	± 0.01	± 0.00	± 0.03	± 0.01	± 0.01	± 0.00
planes <b>b</b> to <b>c</b> <sup>d</sup>	2.30	2.20	2.10	2.06	2.16	2.12	1.95
planes <b>a</b> to <b>c</b> ( <b>e</b> ) <sup>d</sup>	3.49	3.36	3.20	3.16	3.27		
planes <b>a</b> to <b>a</b> <sup>d</sup>	4.70	4.65	4.49	4.47	3.73		
planes <b>c</b> to <b>c</b> <sup>d</sup>	11.66	11.30	10.85	10.78	10.26		

<sup>a</sup> **a–d** are least-squares planes of four atoms each, defined in diagram **56**. <sup>b</sup> Values taken from ref 2. <sup>c</sup> ± values are maxima, not averages. <sup>d</sup> Average of distances of atoms in the first plane from the second least-squares plane.

Table 5. Complexes Isolated and Characterized

Hosts	Guests
<b>MM</b>	
<b>EM</b>	
<b>EE</b>	
<b>PE</b>	
<b>PM</b>	
<b>PP</b>	

The guest of **52** (**PE**⊙-MeC<sub>6</sub>H<sub>4</sub>OMe) is oriented with its long axis aligned closely with the longer polar axis of the host. Inspection of the four stereoviews of this complex (Table 3) indicates the plane of the guest's aryl is close to being in the

plane of two diagonally related *m*-xylyl planes of the bridges. Although we cannot infer this directly from our data, it is very likely that the guest is disordered in the lattice with respect to its two different ends, which means both diastereomeric

complexes appear in the crystal. One diastereomer has the guest's Me in the host's **E** bowl and the guest's MeO in the host's **P** bowl; the other diastereomer has the guest's MeO in the host's **E** bowl and the guest's Me in the **P** bowl. Model (CPK) examination indicates that with new atom connectors in place, these diastereomerically related isomers can interconvert by guest rotation ( $180^\circ$ ) around its shorter equatorial axis with many host-parts' synchronous adjustments, but without disconnecting the bonds. In contrast, the guest in models can rotate ( $90^\circ$ ) much more easily around its longer polar axis to a position in which the guest is coplanar with the alternate set of coplanar diagonally placed C–C<sub>6</sub>H<sub>4</sub>–C parts of the bridges (top views, Table 3). There is no evidence that such a disorder of the guests with respect to the polar axis is present in the four structures reported here.

In **50** (**PE**⊙1,2-(MeO)<sub>2</sub>C<sub>6</sub>H<sub>4</sub>), whose guest non-hydrogen atoms are nearly coplanar, the guest lies roughly in the near-diagonal plane defined by those two diagonally related *m*-xylene bridges whose attached oxygens provide the longer O···O diagonal distance (plane **a**, Table 4, 10.53 Å vs 10.24 Å for the shorter). Both views in Table 3 show that one MeO group of the guest occupies the **E** bowl and the other MeO group is equatorially oriented, but this particular representation is arbitrary, since the arrangement with one MeO group of the guest occupying the **P** bowl and the other MeO group equatorially oriented is equally consistent with the data. These two structures are diastereomers, and since both host and guest are disordered, we cannot know whether only one or both diastereomers are present. In CPK models, these two diastereomers can be easily interconverted by rotation of the guest around a host equatorial axis with little host cooperation. Guest rotation about the host's polar axis is also possible but is more difficult, because spanner and bridge conformational adaptations are required. The pushing of the "oxygen squares" toward a "diagonal arrangement" in the host of this complex reflects the spatial requirements of the equatorially located MeO group of the guest.

We believe that in both **52** (**PE**⊙4-MeC<sub>6</sub>H<sub>4</sub>OMe) and **50** (**PE**⊙1,2-(MeO)<sub>2</sub>C<sub>6</sub>H<sub>4</sub>) the adaptation of host to guest deforms the host from near C<sub>4</sub> symmetry toward near C<sub>2</sub> symmetry. As the crystal grows, it accepts complexes whose hosts are deformed in the same way, a consequence being that the lattice in its growth does not differentiate between the host's (and the guest's) different ends, but does distinguish between guest-induced host diagonal deformations. Thus the only major disorder in the crystal attributable to host–guest shapes arises from the inability of the lattice to differentiate between the two ends of the host and guest. In effect, the two diastereomeric complexes are isostructural. In this connection, CPK models of the two diastereomeric complexes appear to be equally easy to form. In both complexes the guest's aryl hydrogens are able to avoid compressing the spanners' eight near hydrogens only in their diagonal arrangement, which makes them roughly coplanar with the aryl parts of the coplanar (diagonally arranged) bridges.

Of the two bowls of **55** (**EM**⊙4-MeC<sub>6</sub>H<sub>4</sub>OMe), the **M** bowl's tetrol (**10**) possesses C<sub>4</sub> symmetry in CPK models, in contrast to the C<sub>2</sub> symmetry of the **E** bowl tetrol (crystal structure of **11**). In the crystal structure of **55** (**EM**⊙4-MeC<sub>6</sub>H<sub>4</sub>OMe), as in that of **52** (**PE**⊙4-MeC<sub>6</sub>H<sub>4</sub>OMe), the two different ends of both host and guest appear to be averaged, which is the source of the disorder in the lattice. As in **52** (**PE**⊙4-MeC<sub>6</sub>H<sub>4</sub>OMe), the inward-turned hydrogens of the spanning groups in **55** (**EM**⊙4-MeC<sub>6</sub>H<sub>4</sub>OMe) enforce a diagonal arrangement of the guest, which makes the guest roughly coplanar with the aryl parts of the coplanar (diagonally arranged) bridges.

The host in the crystal of **37** (**EE**⊙4-MeC<sub>6</sub>H<sub>4</sub>OMe) also has a center of symmetry. The guest is disordered with respect to its two ends, but not with respect to which of the two diagonals it occupies in the host. Thus the growing lattice differentiates between guest deformations of host associated with its diagonal placement, but not with respect to guest-induced deformations of host at its two ends. Thus the deformations of host by the MeO and Me groups are averaged, and only one set of O···O distances is observed, as in the crystal structures of **52** (**PE**⊙4-MeC<sub>6</sub>H<sub>4</sub>OMe) and **50** (**PE**⊙1,2-(MeO)<sub>2</sub>C<sub>6</sub>H<sub>4</sub>). The fact that the maximum spread in O···O edge distances for the **EE** host (0.65 Å) is more than twice the difference in edge (O···O)<sub>av</sub> of 0.28–0.31 Å between the **PE** and **EE** hosts adds credibility to the above explanation of the disparities in the symmetry properties of host, guest, and crystal lattices in **37** (**EE**⊙4-MeC<sub>6</sub>H<sub>4</sub>OMe), **52** (**PE**⊙4-MeC<sub>6</sub>H<sub>4</sub>OMe), and **50** (**PE**⊙1,2-(MeO)<sub>2</sub>C<sub>6</sub>H<sub>4</sub>). For comparison, in **55** (**EM**⊙4-MeC<sub>6</sub>H<sub>4</sub>OMe), the maximum spread in O···O edge distances is 0.40 Å, and the difference in edge (O···O)<sub>av</sub> for **EM** and **EE** is 0.26 Å.

A measure of host responses in the *equatorial dimension* to changes in spanner and bridge lengths and to guest shapes is found (Table 4) in comparisons of the two O···O diagonal distances. In passing from the **EE** to the two respective **PE** hosts, the average O···O diagonal distances increase by 0.39 and 0.43 Å, respectively. The first and smaller increase of 3.9% represents the change in spanner length (four **E** to four **P** units), while the larger increase of 4.3% also includes the response of the **PE** host to the increased steric demands in its equatorial dimension of 1,2-(MeO)<sub>2</sub>C<sub>6</sub>H<sub>4</sub> over those of 4-MeC<sub>6</sub>H<sub>4</sub>OMe. In passing from **37** (**EE**⊙4-MeC<sub>6</sub>H<sub>4</sub>OMe) to **17** (**9**⊙Me<sub>2</sub>SO), bridge lengths and guest shapes change, but spanners are the same), the average O···O diagonal distance increases by 0.20 Å, or by 2.0%.

The difference in length between the two O···O diagonals (Table 4) divided by their average lengths and multiplied by 100% gives a parameter which measures how much the bowls of the five carceplexes and cavitand **11** deviate from a square to provide a diamond arrangement. The values correlate with structures as follows: **55** (**EM**⊙4-MeC<sub>6</sub>H<sub>4</sub>OMe), 0.4%; **37** (**EE**⊙4-MeC<sub>6</sub>H<sub>4</sub>OMe), 1.2%; **52** (**PE**⊙4-MeC<sub>6</sub>H<sub>4</sub>OMe), 1.1%; **50** (**PE**⊙1,2-(MeO)<sub>2</sub>C<sub>6</sub>H<sub>4</sub>), 2.8%; **17** (**9**⊙Me<sub>2</sub>SO), 13.6%; **11**, 21.4%. The free bowl (**11**) possesses a distinctly diamond arrangement, which is about half suppressed in **17** (**9**⊙Me<sub>2</sub>SO), whose (O(CH<sub>2</sub>)<sub>4</sub>O)<sub>4</sub> bridging groups are conformationally flexible, and whose guest is much too small to exert an influence on the host's shape. In passing from bowl **11** to **50** (**PE**⊙1,2-(MeO)<sub>2</sub>C<sub>6</sub>H<sub>4</sub>), this parameter undergoes a 7-fold drop to 2.8%, which is attributed to the increased rigidity of the (1,3-(OCH<sub>2</sub>)<sub>2</sub>C<sub>6</sub>H<sub>4</sub>)<sub>4</sub> bridges that favors a square arrangement of oxygens. The disk shape of the relatively large 1,2-(MeO)<sub>2</sub>C<sub>6</sub>H<sub>4</sub> guest requires a diagonal arrangement in the host cavity, which distorts the complex 2.8% from the square structure. This distortion essentially disappears in the case of the three 4-MeC<sub>6</sub>H<sub>4</sub>OMe complexes, whose smaller guest is less extended in the diagonal dimensions of the three hosts.

A measure of host responses to changes in spanner lengths and guest shapes in the *axial dimensions* is found in comparisons of the distances (Å) between the two **c** planes of the hemicarceplexes listed in Table 4. The **c** planes are those formed by the four aryl carbon atoms at the two ends of the polar axis of the host's shell (see **56**). These distances vary from 11.66 to 10.26 Å and decrease as follows: **55** (**EM**⊙4-MeC<sub>6</sub>H<sub>4</sub>OMe) > **37** (**EE**⊙4-MeC<sub>6</sub>H<sub>4</sub>OMe) > **52** (**PE**⊙4-MeC<sub>6</sub>H<sub>4</sub>OMe) > **50** (**PE**⊙1,2-(MeO)<sub>2</sub>C<sub>6</sub>H<sub>4</sub>) > **17** (**9**⊙Me<sub>2</sub>SO). The substitution of an **M** for an **E** unit in the first two structures (guest is 4-MeC<sub>6</sub>H<sub>4</sub>-

**Table 6.** Shell Dimensions of 4-MeC<sub>6</sub>H<sub>4</sub>OMe Complexes of Three Known and One Hypothetical Hemicarcerand (**PP**)

distance (Å)	<b>EM</b>	<b>EE</b>	<b>PE</b>	<b>PP</b>
planes <b>c</b> to <b>c</b>	11.66	11.30	10.85	10.40
(O···O) <sub>av</sub> , edge plane <b>a</b>	6.78	7.04	7.32	7.60
(O···O) <sub>av</sub> , diagonals, <b>a</b>	9.58	9.95	10.34	10.73

OMe) increases the polar axis length of the shell by 3.2%, whereas substitution of a **P** for an **E** unit in the second and third structures decreases the polar axis of the shell by 4.0%. Substitution of guest 4-MeC<sub>6</sub>H<sub>4</sub>OMe in host **PE** by guest 1,2-(MeO)<sub>2</sub>C<sub>6</sub>H<sub>4</sub> reduces the polar axial length of the shell by only 0.6%. Substitution of the **EE** host bridges of 1,3-(OCH<sub>2</sub>)<sub>2</sub>C<sub>6</sub>H<sub>4</sub> by O(CH<sub>2</sub>)<sub>4</sub>O, and the 1,2-(MeO)<sub>2</sub>C<sub>6</sub>H<sub>4</sub> guest by Me<sub>2</sub>SO as in **17** (**9**⊙Me<sub>2</sub>SO) reduces the shell length by 9.2%. The maximum difference in the axial shell lengths involves **55** (**EM**⊙4-MeC<sub>6</sub>H<sub>4</sub>OMe), which is 14% greater in this dimension than **17** (**9**⊙Me<sub>2</sub>SO). To the extent data are available, the bridge lengths appear to be more important than either spanner or guest in determining the length of the shell in the axial dimension.

We failed to obtain crystals of **54** (**PP**⊙Me<sub>3</sub>CPh) suitable for X-ray structure determination. The interpretations of the crystal structures of **37** (**EE**⊙4-MeC<sub>6</sub>H<sub>4</sub>OMe) and **52** (**PE**⊙4-MeC<sub>6</sub>H<sub>4</sub>OMe) allow the structural parameters of a hypothetical **PP**⊙4-MeC<sub>6</sub>H<sub>4</sub>OMe to be estimated by linear extrapolation assuming the **bo-su** conformation for both bowls of the latter, which is observed for the **P** bowl of **52** (**PE**⊙4-MeC<sub>6</sub>H<sub>4</sub>OMe) (see Table 6). The lengths of the polar axes as measured by **c-c** distances exceed the lengths of the equatorial axes as measured by (O···O)<sub>av</sub> diagonal distances in planes **a** (see **56**) by the following amounts (Å): **37** (**EE**⊙4-MeC<sub>6</sub>H<sub>4</sub>OMe), 1.35; **52** (**PE**⊙4-MeC<sub>6</sub>H<sub>4</sub>OMe), 0.51; hypothetical **PP**⊙4-MeC<sub>6</sub>H<sub>4</sub>OMe, -0.33 Å. This near-spherical shape of **PP** host's hypothetical shell is visible in CPK models. The parameters for **55** (**EM**⊙4-MeC<sub>6</sub>H<sub>4</sub>OMe) are included in Table 6 for comparison purposes.

The fact that the hypothetical **PP** host's equatorial axis exceeds the polar axis in length suggests possible alignments of the longest axis of guests along equatorial axes in the **PP** host. Although this possibility may be encountered in future crystal structures, it is unlikely for guests whose long ends are bulky, such as 1,4-(MeO)<sub>2</sub>C<sub>6</sub>H<sub>4</sub>, but more likely with guests whose long ends are slim, such as 1,4-(HO)<sub>2</sub>C<sub>6</sub>H<sub>4</sub>. The polar bowls are more spacious than the equatorial border regions, which are somewhat encumbered by inward-turned hydrogens of the spanner groups.

**Correlations of <sup>1</sup>H NMR Spectra with Structures of the Hemicarceplexes.** The Δδ values for the guests of **1-9** are all positive, ranging from a high of 4.29 ppm for the (a)-(CH<sub>3</sub>O) protons of **26** (**EM**⊙1,2,3-(MeO)<sub>3</sub>C<sub>6</sub>H<sub>3</sub>) to a low of 0.00 ppm for the (b)-CH<sub>3</sub> protons of **32** (**EE**⊙PhCH(Me)CH<sub>2</sub>Me(b)) (Table 2). High magnitudes reflect proximity of the guest protons to the shielding faces of the eight aryl groups that define the two polar caps of the hosts, and low magnitudes locate guest protons in the equatorial regions of the hosts. Models of **15** (**7**⊙Me<sub>2</sub>SO), **16** (**8**⊙Me<sub>2</sub>SO), and **17** (**9**⊙Me<sub>2</sub>SO) show that one methyl must occupy a polar cap while the second is equatorially located. The singlet signals show these protons are averaging rapidly on the NMR time scale to provide Δδ = 3.26 for **17** (**9**⊙Me<sub>2</sub>SO), somewhat higher than the respective 2.92 and 2.95 ppm values observed for **15** (**7**⊙Me<sub>2</sub>SO) and **16** (**8**⊙Me<sub>2</sub>SO), whose hosts differ only in their "feet". As predicted by model examination, changes in the remote feet have little effect on the cavity and guest. Models of **17** (**9**⊙Me<sub>2</sub>SO) suggest the ethylene spanners of the host widen the polar caps allowing

the methyls of the guest to more deeply penetrate this highly shielding region than do the methylene spanners of **7** and **8**.

Intramolecular compacting of protons as in the guests CBr<sub>2</sub>-HCBr<sub>2</sub>H and the methyls of MeCOCMe<sub>3</sub>, Me<sub>2</sub>C(OH)C(OH)Me<sub>2</sub>, Me<sub>3</sub>CPh, PhCH(Me)CH<sub>2</sub>Me, 1,2-Me<sub>2</sub>C<sub>6</sub>H<sub>4</sub>, and 1,2-(MeO)<sub>2</sub>C<sub>6</sub>H<sub>4</sub> all provide Δδ values that range from 0.00 to 2.51 ppm. Methyl protons of guests containing unhindered aryl methyls such as MePh, 1,3-Me<sub>2</sub>C<sub>6</sub>H<sub>4</sub>, 1,4-Me<sub>2</sub>C<sub>6</sub>H<sub>4</sub>, and aryl acetyl guests such as MeCOPh, 2-MeCOC<sub>6</sub>H<sub>4</sub>Me, 2-MeCOC<sub>6</sub>H<sub>4</sub>Cl, 2-MeCOC<sub>6</sub>H<sub>4</sub>-Br, and 2-MeCOC<sub>6</sub>H<sub>4</sub>OMe deeply penetrate the shielding polar caps to give Δδ values that range from 2.93 to 3.47 ppm. Aryl protons *para* to the substituent in monosubstituted benzenes as in guests MePh, Me<sub>3</sub>CPh, and MeCOPh also occupy the polar caps to provide Δδ values of 3.29 to 3.92 ppm. Other aryl Δδ values are scattered between 0.48 and 3.17 ppm, depending on their placements in both guest and host.

In CPK models the conformations of (OCH<sub>2</sub>O)<sub>4</sub> and (OCH<sub>2</sub>-CH<sub>2</sub>O)<sub>4</sub> spanners are pretty well fixed, but those of (OCH<sub>2</sub>-CH<sub>2</sub>CH<sub>2</sub>O)<sub>4</sub> are fluxional. Examination of models that combine rigid **M** or **E** units with flexible **P** units indicates the rigid units must impose shapes on the flexible units when the two kinds are coupled at their lips in the same hemicarcerand, as in **PM**, **PE**, and **EM**. Comparisons of Δδ values for guests incarcerated in different kinds of hosts support this supposition. Hosts **EE** and **PE** complexed with the same guest produce similar Δδ values (compare those of Me<sub>3</sub>CPh, MeCOPh, 1,2-(MeO)<sub>2</sub>C<sub>6</sub>H<sub>4</sub>, 4-MeC<sub>6</sub>H<sub>4</sub>OMe, and coumarin in Table 2). Similarly hosts **MM** and **PM** (and even **EM** if the two sets of <sup>3</sup>H protons are averaged) complexed with 1,2,3-(MeO)<sub>3</sub>C<sub>6</sub>H<sub>3</sub> give similar Δδ values for the guest protons. These correlations also indicate that the **P** unit in **45** (**PE**⊙Me<sub>3</sub>CPh), **47** (**PE**⊙MeCOPh), **50** (**PE**⊙(MeO)<sub>2</sub>C<sub>6</sub>H<sub>4</sub>), and **53** (**PM**⊙(MeO)<sub>3</sub>C<sub>6</sub>H<sub>3</sub>) possess the **bo-su** or a like conformation. This conclusion was reached before the crystal structure of **52** (**PE**⊙MeC<sub>6</sub>H<sub>4</sub>OMe) became available. Complexation-decomplexation probably occurs through the **bi-su** or equivalent conformation, whose hosts in models allow these guests to enter and depart their complexes easily.

Neither **MM** nor **PP** formed isolable complexes with coumarin or 1,2-(MeO)<sub>2</sub>C<sub>6</sub>H<sub>4</sub>, but both **EE** and **PE** formed isolable complexes with each guest. The Δδ values of **34** (**EE**⊙1,2-(MeO)<sub>2</sub>C<sub>6</sub>H<sub>4</sub>) and **50** (**PE**⊙1,2-(MeO)<sub>2</sub>C<sub>6</sub>H<sub>4</sub>) protons range from 1.97 ppm to 2.17 ppm, which suggests these guests largely occupy the equatorial region of the host. Unlike models with **M** unit-dominated cavities, those with **E** unit-dominated cavities possess equatorial dimensions large enough to accommodate simple *ortho*-disubstituted benzenes. The Δδ values of **38** (**EE**⊙coumarin) and **46** (**PE**⊙coumarin) guest protons range from 3.22 to 3.50 ppm, which indicates that they are located in the polar regions, with the long axes of host and guest roughly aligned.

The successful assembly of models of the five complexes of 1,2,3-(MeO)<sub>3</sub>C<sub>6</sub>H<sub>3</sub> depends on distribution of the guest's 1,3-(CH<sub>3</sub>O)<sub>2</sub> groups (<sup>3</sup>H of Table 2) into the two polar caps of the cavity, with the 2-CH<sub>3</sub>O group being essentially coplanar with its attached aryl. That plane is oriented half way between coincidence with the polar and equatorial axes of the host (model examination). This general structure is consistent with the relatively high Δδ values of the <sup>3</sup>H protons that range from 4.29 ppm in **26** (**EM**⊙1,2,3-(MeO)<sub>3</sub>C<sub>6</sub>H<sub>3</sub>) to 3.09 ppm in **51** (**PE**⊙1,2,3-(MeO)<sub>3</sub>C<sub>6</sub>H<sub>3</sub>) and the relatively low Δδ values of the ArH protons (<sup>c</sup>H and <sup>d</sup>H, Table 2), which range from 0.47 to 1.96 ppm. The <sup>b</sup>H protons of the central methoxyl vary only from Δδ = 0.94 to 1.01 ppm, which shows the hydrogens occupy the low-shielding equatorial regions of the cavities. Particularly striking is the fact that only the host with the

smallest cavity composed of two unlike hemispheres, **EM**, provides *two different signals* for its guest's  $^1\text{H}$  protons, one at  $\delta = -0.44$  (methyl inserted into the **E** unit), and the second at  $\delta = 0.32$  ppm (methyl inserted into the **M** unit) to give  $\Delta\delta$  values of 4.29 and 3.53 ppm, respectively. The existence of these two signals indicates that the *rate of equilibration of the two terminal methoxyl group protons of the guest between the two unlike environments in the host cavities is slow on the  $^1\text{H}$  NMR time scale in  $\text{CDCl}_3$  at 25 °C*. In contrast, **51** (**PE**⊙1,2,3-(MeO) $_3$ C $_6$ H $_3$ ) exhibits an equilibrated signal at  $\delta = 0.76$  ( $\Delta\delta = 3.09$  ppm), consistent with the larger cavity of **PE** compared with that of **EM**. Likewise at 25 °C in  $\text{CDCl}_3$  only one set each for Me and MeO signals is observed in the spectrum of **52** (**PE**⊙4-MeC $_6$ H $_4$ OMe), suggesting the diastereoisomers are equilibrating rapidly on the  $^1\text{H}$  NMR time scale at this temperature.

The most easily identified and characteristic changes in signals of hosts **1–6** upon complexation are those due to the aryl  $^1\text{H}$  proton of the 1,3-(OCH $_2$ ) $_2$ C $_6$ H $_4$  bridges, which in models generally point toward the guest. The  $\delta$  values in  $\text{CDCl}_3$  for  $^1\text{H}$  of the five free hosts available (uncomplexed **PM** was never obtained) became less shielded as the spanners became longer as follows: **MM**,  $\delta = 7.46$ ; **EM**,  $\delta = 7.60$ ; **EE**,  $\delta = 7.88$ ; **PE**,  $\delta = 7.95$ ; and **PP**,  $\delta = 8.02$  ppm, the total spread in values equalling 0.56 ppm. Aside from those of **24** (**MM**⊙3,4,5-(MeO) $_3$ C $_6$ H $_2$ OH), the hosts'  $\Delta\delta$  values for their complexes varied between  $-0.21$  and  $0.21$  ppm. The only generalization extractable from the data of Table 2 about the latter is that those guests which most rigidly extend in three dimensions provide the largest magnitudes in  $\Delta\delta$  values (either positive or negative). Examples are **19** (**MM**⊙MeCOCMe $_3$ ) ( $\Delta\delta = -0.21$ ), **21** (**MM**⊙PhCMe $_3$ ) ( $\Delta\delta = +0.21$ ), **26** (**EM**⊙1,2,3-(MeO) $_3$ C $_6$ H $_3$ ) ( $\Delta\delta = +0.20$ ), and **36** (**EE**⊙1,2,3-(MeO) $_3$ C $_6$ H $_3$ ) ( $\Delta\delta = +0.19$  ppm). Model examination of hosts **1–6** shows that in extremes, the aryl planes of the bridges can twist as much as 45° to either side of the symmetrical conformations shown in top views in Table 3. Given the larger variation in  $\delta$  values among the hosts themselves (0.56 ppm) than is observed in the spread of  $\Delta\delta$  with the guest changes (0.42 ppm), it is obvious that the many cancelling effects of guest and host structures on their  $^1\text{H}$  NMR spectra combine to confound further analysis.

Unlike any other hemicarceplex prepared to date, **22** (**MM**⊙Ph $_2$ O) provides an  $^1\text{H}$  NMR spectrum which indicates the guest does not rotate about any host axis rapidly on the NMR time scale. The awkward shape, rigidity, and large size (C $_{12}$ H $_{10}$ O) of this guest makes CPK models of **22** (**MM**⊙Ph $_2$ O) difficult to assemble, and highly dissymmetric. The crowding of two phenyls and an oxygen into a noncomplementary inner phase provides the guest with little mobility, which modifies the magnetic environment of the host's proximate protons in a nonaveraged way, greatly complicating its spectrum. The eight Ar-*H* protons of the cavitand hemispheres provide three different singlets (about 2:1:1 intensity), showing nonequivalence of magnetic fields in the polar regions of the shell. One four-proton singlet of the bridges' OCH $_2$ Ar occurs at 4.96 ppm, but the other 12 benzyl protons appear as a complex multiplet ( $\delta$  4.66–4.96 ppm), which also includes the eight methines. The spanner OCH $_2$ O signals which usually appear as doublets are multiplets (OCH $_2$ O inner,  $\delta$  4.26, 8 H and OCH $_2$ O outer,  $\delta$  5.51, 8 H), which indicates the two bowls have different magnetic environments.

**Qualitative Decomplexation Rates: Comparisons of complexes of **EE** and **PE**.** Because of the generally large  $\Delta\delta$  (ppm)  $^1\text{H}$  NMR values, order of magnitude comparisons of the half-lives for decomplexation were easily made in  $\text{CDCl}_3$  at 25 °C.

The half-lives varied from extremes of a few minutes to months. For example  $t_{1/2} \approx 0.33$  h for **47** (**PE**⊙MeCOPh), and  $t_{1/2} \approx 48$  h for **39** (**EE**⊙MeCOPh), so **47** (**PE**⊙MeCOPh)  $\gg$  **39** (**EE**⊙MeCOPh) in decomplexation rate. Complexes **MM**⊙MeCOPh and **PP**⊙MeCOPh are undoubtedly unstable to isolation. Both **40** (**EE**⊙2-MeC $_6$ H $_4$ COMe) and **48** (**PE**⊙2-MeC $_6$ H $_4$ COMe) are more kinetically stable than their corresponding complexes with MeCOPh, and **40** (**EE**⊙2-MeC $_6$ H $_4$ COMe)  $>$  **48** (**PE**⊙2-MeC $_6$ H $_4$ COMe) in decomplexation rate. In contrast, **52** (**PE**⊙4-MeC $_6$ H $_4$ OMe)  $>$  **37** (**EE**⊙4-MeC $_6$ H $_4$ OMe) in decomplexation rate. For the planar guest, coumarin, **46** (**PE**⊙coumarin)  $>$  **38** (**EE**⊙coumarin) in decomplexation rate, since **PE** is much more conformationally flexible than **EE**. When the rate for decomplexation of differently 2-substituted acetophenones of **EE** complexes are compared, **40** (**EE**⊙2-MeC $_6$ H $_4$ COMe)  $>$  **41** (**EE**⊙2-ClC $_6$ H $_4$ COMe)  $>$  **42** (**EE**⊙2-BrC $_6$ H $_4$ COMe)  $\approx$  **43** (**EE**⊙2-MeOC $_6$ H $_4$ COMe). Comparison of the rates for decomplexation of the isomeric xylenes provides the order, **29** (**EE**⊙1,3-Me $_2$ C $_6$ H $_4$ )  $\gg$  **30** (**EE**⊙1,4-Me $_2$ C $_6$ H $_4$ )  $>$  **28** (**EE**⊙1,2-Me $_2$ C $_6$ H $_4$ ). Solutions in  $\text{CDCl}_3$  at 25 °C of **EE** complexes with Me $_3$ CPh, 1,2-(MeO) $_2$ C $_6$ H $_4$ , 1,2,3-(MeO) $_3$ C $_6$ H $_3$ , 2-ClC $_6$ H $_4$ CO $_2$ Me, and of **PE** complexes with Me $_3$ CPh, 1,2-(MeO) $_2$ C $_6$ H $_4$  and 1,2,3-(MeO) $_3$ C $_6$ H $_3$  are stable indefinitely.

These qualitative orders for rates of decomplexation when taken in sum provide the following overall generalizations: (1) The kinetic stability orders for hemicarceplexes whose hosts involve 1,3-(OCH $_2$ ) $_2$ C $_6$ H $_4$  bridges (**1–6**) vary widely with changes in the spanners of the hosts as well as with changes in the shapes, sizes, and electronic character of their guests. With some guests, **EE** complexes are more kinetically stable than their **PE** counterparts, but with others, the opposite order is observed. (2) When guests reach 10–13 heavy atoms in size, which are distributed substantially and rigidly in three dimensions (e.g., more than coumarin), their formable complexes with **1–6** are stable in  $\text{CDCl}_3$  at 25 °C. Examples of such guests are Me $_3$ CPh (complexes **MM**, **EM**, **EE**, **PE**, and **PP**), and 1,2,3-(MeO) $_3$ C $_6$ H $_3$  (complexes **MM**, **EM**, **EE**, **PE**, and **PM**). (3) The complex with the largest guest is **22** (**MM**⊙Ph $_2$ O), whose guest contains 13 heavy atoms and 10 hydrogens. The increase in the multiplicity of both host and guest  $^1\text{H}$  NMR signals of this complex indicates the guest cannot rotate rapidly on the NMR time scale around any of its host's axes at ambient temperature. Interestingly, **MM** also forms complexes stable to isolation with the smallest guests (CB $_2$ HCB $_2$ H, Me $_3$ CCOMe, and Me $_2$ C-(OH)C(OH)Me $_2$ ), attesting to the importance in obtaining stable complexes of the distribution of the guest's bulk in all three dimensions.

**Summary.** Forty one-to-one complexes involving nine hosts and 24 guests have been prepared and characterized. Most of them were prepared by heating host in the presence of large excesses of guest. The guests range in numbers of non-hydrogen atoms from four to 13 atoms. Crystal structures of **55** (**EM**⊙4-MeC $_6$ H $_4$ OMe), **37** (**EE**⊙4-MeC $_6$ H $_4$ OMe), **52** (**PE**⊙4-MeC $_6$ H $_4$ OMe), and **50** (**PE**⊙1,2-(MeO) $_2$ C $_6$ H $_4$ ) were determined. Values of  $\Delta\delta$  (difference in chemical shift values of guest proton signals, free and incarcerated) correlate well with expectations based on molecular model examination guided by crystal structures. The **P** bowls are conformationally mobile, but when bonded rim-to-rim with relatively rigid **E** or **M** bowls through 1,3-(OCH $_2$ ) $_2$ C $_6$ H $_4$  bridges, the **P** bowls assume a **bo-su** conformation. Guests Me $_3$ CPh and 1,2,3-(MeO) $_3$ C $_6$ H $_3$  each formed complexes with five of **1–6** hosts. High structural recognition was shown by **EE** and **PE** in the rates of complexing and decomplexing *ortho*-, *meta*- and *para*-isomers of disubstituted benzenes. Only the host with the narrowest cavity composed

of two unlike bowls (**EM**) prevents the two distant Me groups of 1,2,3-(MeO)<sub>3</sub>C<sub>6</sub>H<sub>3</sub> from replacing one another rapidly at 25 °C on the <sup>1</sup>H NMR time scale in CDCl<sub>3</sub>. The host with the narrowest cavity, **MM**, formed stable complexes with the largest (Ph<sub>2</sub>O) and smallest guest (Br<sub>2</sub>CHCHBr<sub>2</sub>), pointing to the importance of shape in host–guest relationships. At ambient temperature, **22** (**MM**⊙Ph<sub>2</sub>O) is unique since its guest appears immobilized with respect to molecular rotations inside its host.

## Experimental Section

**General.** Organic compounds used in complexation experiments were purchased from Aldrich Chemical Company unless otherwise noted and were of the highest purity available. All reactions were conducted under an atmosphere of argon, unless indicated otherwise. A Bruker ARX 500 MHz spectrometer was used to record <sup>1</sup>H NMR spectra. Spectra were taken in CDCl<sub>3</sub> and were referenced to residual CHCl<sub>3</sub> at 7.26 ppm. FAB MS were determined on a ZAB SE instrument with 3-nitrobenzyl alcohol (NOBA) as a matrix. Analytical and preparative thin-layer chromatography was performed on E. Merck glass-backed plates (silica gel 60, F<sub>254</sub>, 0.25 mm and 0.5 mm thicknesses).

**23** (**MM**⊙1,2,3-(MeO)<sub>3</sub>C<sub>6</sub>H<sub>3</sub>). **Procedure A.** To a pyrex test tube equipped with an inert gas inlet was added 20 mg (0.009 mmol) of **MM** and 2.0 g (11.9 mmol) of 1,2,3-(MeO)<sub>3</sub>C<sub>6</sub>H<sub>3</sub>. The mixture was heated at 160 °C for 2 days, cooled to ~80 °C and poured into 60 mL of MeOH. The solid was filtered, dried in vacuo, and purified by preparative TLC (4:1 CH<sub>2</sub>Cl<sub>2</sub>–hexane as eluent) to give 16 mg (74%) of **23**: <sup>1</sup>H NMR δ –0.11 (s, 6 H, OCH<sub>3</sub>), 0.94 (t, *J* = 7.1 Hz, 24 H, CH<sub>2</sub>CH<sub>3</sub>), 1.32–1.54 (m, 48 H, (CH<sub>2</sub>)<sub>3</sub>), 2.20 (m, 16 H, CHCH<sub>2</sub>), 2.85 (s, 3 H, OCH<sub>3</sub>), 4.26 (d, *J* = 7.1 Hz, 8 H, inner OCH<sub>2</sub>O), 4.81 (m, 24 H, ArCH<sub>2</sub> and CH methine), 5.18 (d, *J* = 8.5 Hz, 2 H, guest ArH), 5.58 (d, *J* = 7.1 Hz, 8 H, outer OCH<sub>2</sub>O), 6.43 (t, *J* = 8.5 Hz, 1 H, guest ArH), 6.92 (s, 8 H, ArH), and 7.18–7.34 (m, 16 H, ArH); MS FAB *m/e* 2339 (complex<sup>+</sup>, 100), *m/e* 2170 (**MM**, 15). Anal. Calcd for C<sub>136</sub>H<sub>152</sub>O<sub>24</sub>·C<sub>9</sub>H<sub>12</sub>O<sub>3</sub>: C, 74.46; H, 7.07. Found: C, 74.58; H, 6.93.

**31** (**EE**⊙1,2,4-(Me)<sub>3</sub>C<sub>6</sub>H<sub>3</sub>). **Procedure B.** A mixture of 20 mg (0.009 mmol) of **EE** in 2 mL of 98% 1,2,4-(Me)<sub>3</sub>C<sub>6</sub>H<sub>3</sub> under argon was heated 3 days at 160 °C. The mixture was cooled to ~80 °C and poured into 60 mL of MeOH. The product was collected on a fine-sintered glass funnel and dried at 10<sup>–5</sup> Torr (25 °C) for 18 h to give 17 mg (81%) of **31** as a white solid: <sup>1</sup>H NMR δ –1.31 (s, 3 H, guest CH<sub>3</sub>), –1.08 (s, 3 H, guest CH<sub>3</sub>), 0.90 (t, *J* = 6.9 Hz, 24 H, CH<sub>2</sub>CH<sub>3</sub>), 1.18–1.60 (m, 51 H, (CH<sub>2</sub>)<sub>3</sub>, guest CH<sub>3</sub>), 2.05–2.22 (m, 16 H, CHCH<sub>2</sub>), 3.52–3.60 (m, 16 H, inner OCH<sub>2</sub>CH<sub>2</sub>O), 3.78–3.98 (m, 16 H, outer OCH<sub>2</sub>CH<sub>2</sub>O), 4.68 (s, 1 H, guest ArH), 5.06–5.20 (m, 24 H, ArCH<sub>2</sub>, CH methine), 5.75 (d, *J* = 6.7 Hz, 1 H, guest ArH), 6.88–7.30 (m, 20 H, ArH), 7.78 (s, 4 H, ArH); MS FAB *m/e* 2404 (100), 2282 (60). Anal. Calcd for C<sub>144</sub>H<sub>168</sub>O<sub>24</sub>·C<sub>9</sub>H<sub>12</sub>: C, 76.47; H, 7.55. Found: C, 76.72; H, 7.56.

A similar experiment involving 20 mg (0.009 mmol) of **EE** and 2 mL of 98% 1,3,5-(Me)<sub>3</sub>C<sub>6</sub>H<sub>3</sub> (150 °C for 3 days) gave 13 mg (62%) of **31**. The physical properties and <sup>1</sup>H NMR spectrum of this material were identical with the complex isolated from **EE** and 1,2,4-(Me)<sub>3</sub>C<sub>6</sub>H<sub>3</sub>.

**38** (**EE**⊙Coumarin). **Procedure C.** A mixture of 20 mg (0.009 mmol) of **EE**, 2 g (13.7 mmol) of coumarin, and 2 g of Ph<sub>2</sub>O was heated 4 days at 185 °C. The solution was cooled to ~80 °C, diluted with 9:1 MeOH–CHCl<sub>3</sub>, filtered, and purified by preparative TLC (4:1 CH<sub>2</sub>Cl<sub>2</sub>–hexane as eluent) to give 10 mg (47%) of **38**: <sup>1</sup>H NMR δ 0.90 (t, *J* = 7.0 Hz, 24 H, CH<sub>2</sub>CH<sub>3</sub>), 1.18–1.56 (m, 48 H, (CH<sub>2</sub>)<sub>3</sub>), 2.08–2.18 (m, 16 H, CHCH<sub>2</sub>), 2.92 (d, *J* = 9.5 Hz, 1 H, guest vinyl H), 3.33–3.46 (m, 16 H, inner OCH<sub>2</sub>CH<sub>2</sub>O), 3.77–3.88 (m, 16 H, outer OCH<sub>2</sub>CH<sub>2</sub>O), 3.93 (m, 2 H, guest ArH), 4.28 (d, *J* = 9.5 Hz, 1 H, guest vinyl H), 5.08–5.22 (m, 24 H, ArCH<sub>2</sub>, CH methine), 6.49 (m, 1 H, guest ArH), 7.02–7.32 (m, 20 H, ArH), 7.98 (s, 4 H, ArH); MS FAB *m/e* 2430 (60), 2282 (100). Anal. Calcd for C<sub>144</sub>H<sub>168</sub>O<sub>24</sub>·C<sub>9</sub>H<sub>6</sub>O<sub>2</sub>: C, 75.65; H, 7.22. Found: C, 75.28; H, 7.24.

**41** (**EE**⊙2-ClC<sub>6</sub>H<sub>4</sub>COMe). A mixture of 20 mg (0.009 mmol) of **EE** and 2 mL of 97% 2-ClC<sub>6</sub>H<sub>4</sub>COMe was heated 4 days at 150 °C. Application of procedure B gave 15 mg (70%) of **41**: <sup>1</sup>H NMR δ –0.69 (s, 3 H, COCH<sub>3</sub>), 0.90 (t, *J* = 7 Hz, 24 H, CH<sub>2</sub>CH<sub>3</sub>), 1.18–1.52 (m, 48 H, (CH<sub>2</sub>)<sub>3</sub>), 2.07–2.18 (m, 16 H, CHCH<sub>2</sub>), 3.46–3.60 (m, 16 H,

inner OCH<sub>2</sub>CH<sub>2</sub>O), 3.88–3.98 (m, 16 H, outer OCH<sub>2</sub>CH<sub>2</sub>O), 4.42 (d, *J* = 8.1 Hz, 1 H, guest ArH), 5.07–5.20 (m, 24 H, ArCH<sub>2</sub>, CH methine), 5.98 (d, *J* = 7.9 Hz, 1 H, guest ArH), 6.33 (t, *J* = 7.4 Hz, 1 H, guest ArH), 7.02–7.28 (m, 20 H, ArH), 7.84 (s, 4 H, ArH); MS FAB *m/e* 2437 (100), 2282 (75). Anal. Calcd for C<sub>144</sub>H<sub>168</sub>O<sub>24</sub>·C<sub>8</sub>H<sub>7</sub>ClO: C, 74.90; H, 7.24. Found: C, 74.66; H, 7.01.

A similar experiment with 20 mg (0.009 mmol) of **EE** and 2 mL of 98% 4-ClC<sub>6</sub>H<sub>4</sub>COMe (150 °C, 4 days) gave 14 mg of a white solid identified as a mixture of **EE** and **41** (by TLC and <sup>1</sup>H NMR). Integration of the singlet absorption in the *m*-xylyl bridge (7.84 ppm for **41** and 7.88 ppm for **EE**) gave 55% of complex and 45% **EE**.

Reaction of 20 mg (0.009 mmol) of **EE** and 2 mL of 98% 3-ClC<sub>6</sub>H<sub>4</sub>COMe (150 °C, 4 days) gave 12 mg of a white solid. Two compounds were observed by TLC (4:1 CH<sub>2</sub>Cl<sub>2</sub>–hexane) which were identified as **EE** (~60%) and **EE**⊙3-ClC<sub>6</sub>H<sub>4</sub>COMe by <sup>1</sup>H NMR and MS. The <sup>1</sup>H NMR spectrum of the mixture exhibited a singlet at –1.0 ppm attributed to the MeCO of the complexed guest (note: the MeCO in **41** appears at –0.69 ppm) and the aryl singlet at 7.84 ppm is assigned to the *m*-xylyl bridges in the complex. The FAB MS of the mixture gave *m/e* 2437 (30) for **EE**⊙3-ClC<sub>6</sub>H<sub>4</sub>COMe in addition to *m/e* 2282 (100) for **EE**.

**32** (**EE**⊙PhCH(Me)CH<sub>2</sub>Me). A mixture of 20 mg (0.009 mmol) of **EE** and 2 mL of PhCH(Me)CH<sub>2</sub>Me was heated 3 days at 160 °C. Application of procedure B gave 15 mg (70%) of **32**: <sup>1</sup>H NMR δ –0.87 (s (br), 3 H, ArCHCH<sub>3</sub> of guest), 0.81 (t, *J* = 5.9 Hz, 3 H, CH<sub>2</sub>CH<sub>3</sub> of guest), 0.91 (t, *J* = 7.0 Hz, 24 H, CH<sub>2</sub>CH<sub>3</sub>), 1.17–1.63 (m, 50 H, (CH<sub>2</sub>)<sub>3</sub>, CH<sub>2</sub> of guest), 2.05–2.16 (m, 16 H, CHCH<sub>2</sub>), 3.50–3.60 (m, 16 H, inner OCH<sub>2</sub>CH<sub>2</sub>O), 3.85–3.98 (m, 16 H, outer OCH<sub>2</sub>CH<sub>2</sub>O), 4.24 (t, *J* = 5.9 Hz, 1 H, guest ArH), 5.04–5.22 (m, 24 H, ArCH<sub>2</sub>, CH methine), 5.55 (t, *J* = 5.9 Hz, 2 H, guest ArH), 6.17 (d, *J* = 5.9 Hz, 2 H, guest ArH), 6.98–7.30 (m, 20 H, ArH), 7.93 (s, 4 H, ArH); MS FAB *m/e* 2404 (complex – CH<sub>3</sub>, 35), *m/e* 2282 (100). Anal. Calcd for C<sub>144</sub>H<sub>168</sub>O<sub>24</sub>·C<sub>10</sub>H<sub>14</sub>·3H<sub>2</sub>O: C, 74.85; H, 7.67. Found: C, 74.43; H, 7.31.

**33** (**EE**⊙Me<sub>3</sub>CPh). The reaction of **EE** and 99% Me<sub>3</sub>CPh (procedure B) gave free **EE**, **32** (**EE**⊙PhCH(Me)CH<sub>2</sub>Me) and **33** in the relative amounts 55:30:15 (150 °C, 3 days) and 40:15:45 (160 °C, 11 days), respectively. GC-MS analysis of Me<sub>3</sub>CPh indicated ~2% PhCH(Me)CH<sub>2</sub>Me present as impurity which accounts for the formation of the isomeric complex.<sup>7</sup>

**Preparations of 22** (**MM**⊙Ph<sub>2</sub>O). A mixture of 0.30 g (0.34 mmol) of tetrol **10**, 0.30 g (1.7 mmol) of 1,3-(ClCH<sub>2</sub>)<sub>2</sub>C<sub>6</sub>H<sub>4</sub>, 4 g of Cs<sub>2</sub>CO<sub>3</sub>, 10 mL of Ph<sub>2</sub>O and 190 mL of *N*-methylpyrrolidinone was stirred at 65 °C under argon for 24 h. A 0.3 g (1.7 mmol) additional portion of the dichloride was added and stirring was continued for 36 h. The solvent was evaporated under vacuum, the residue was partitioned between CHCl<sub>3</sub> and 10% aqueous NaCl, and the CHCl<sub>3</sub> layer was dried (MgSO<sub>4</sub>), concentrated to ~5 mL and MeOH (300 mL) was added. The crude product that precipitated was collected, dissolved in 10 mL of CHCl<sub>3</sub>, and flash chromatographed on 100 g of silica gel. The column was eluted with 7:3 (v) CH<sub>2</sub>Cl<sub>2</sub>–hexane and CH<sub>2</sub>Cl<sub>2</sub> to provide 130 mg of a 7:3 mixture (<sup>1</sup>H NMR) of **MM** and **22**. The ratio of the two products was determined by integrating the hydrogens of the inner and outer methylenes of the spanners and the singlet of the Ar–<sup>3</sup>H in the bridging 1,3-(OCH<sub>2</sub>)<sub>2</sub>C<sub>6</sub>H<sub>4</sub> units. These results provide calculated shell closure yields of ~24% for **MM** and ~10% for **22**. These compounds have the same *R<sub>f</sub>* in a variety of CH<sub>2</sub>Cl<sub>2</sub>–hexane mixtures on TLC. To separate the host from the complex, 40 mg of the mixture was dissolved in 2.0 g of Ph<sub>2</sub>O and 2.0 g of Me<sub>2</sub>C(OH)C(OH)Me<sub>2</sub>, and the solution was heated at 150 °C for 2 days. The mixture was poured into 90 mL of MeOH, the precipitate was filtered and washed, and the solid mixture of **22** and **20** (**MM**⊙Me<sub>2</sub>C(OH)C(OH)Me<sub>2</sub>) was separated by preparative TLC (70:30 CH<sub>2</sub>Cl<sub>2</sub>–hexane) to give 6 mg of **22** and 25 mg of **20**, the former having the higher *R<sub>f</sub>*.

When **MM** was heated in Ph<sub>2</sub>O at 180 °C for 7 days, a mixture of 5% of **22** and 95% of **MM** was obtained, as identified by MS and <sup>1</sup>H NMR spectra. When **MM** and a 1:1 (w/w) mixture of Ph<sub>2</sub>O and coumarin were heated at 165 °C for 2 d, a 60% yield of a 3:1 mixture

(7) Analysis of Me<sub>3</sub>CPh was performed on a Hewlett-Packard Model 5890 instrument. The authors thank Professor Joan S. Valentine and Ms. Diana Wertz for assistance in this measurement.

( $^1\text{H}$  NMR analysis) of **MM** and **22** was isolated and identified by  $^1\text{H}$  NMR and MS techniques.

**Decomplexation of Complexes.** Solutions of 4 mg of complex in 0.5 mL of  $\text{CDCl}_3$  were placed in NMR tubes and spectra were recorded on a Bruker ARX 500 MHz spectrometer at 25 °C with periodic recording of spectra. Integration of the aryl singlet (*m*-xylyl bridging group of host) for free host and complex was used to follow the decomplexation. Using this method the half-life (25 °C) for decomplexation of **29** ( $\text{EE}\odot 1,3\text{-Me}_2\text{C}_6\text{H}_4$ ) was  $\sim 3$  h and that of **30** ( $\text{EE}\odot 1,4\text{-Me}_2\text{C}_6\text{H}_4$ ) was 13 days. The decomplexation of **28** ( $\text{EE}\odot 1,2\text{-Me}_2\text{C}_6\text{H}_4$ ) was about 10% complete after 30 days.

**Crystal Structures. General.** The crystal structure of each of the four compounds (**37**, **50**, **52** and **55**) belongs to the triclinic space group  $\text{P}\bar{1}$ , and each host lies on a center of symmetry. There is some disorder in all four structures since, although host **2** (structure **37**) is centrosymmetric, the other hosts and all the guests are not centrosymmetric. All structures were solved by direct methods.<sup>8a</sup> Final refinements ( $F^2$ ) were performed with SHELXL-93.<sup>8b</sup> All non-hydrogen atoms were refined with isotropic displacement parameters. All hydrogen atoms were geometrically located and refined riding or in rigid groups with fixed C–H distances (0.93–0.97 Å). The displacement parameter for each H was fixed at 1.5 (Me) or 1.2 (all other H) times that of the attached C or O atom.

The crystal structure of **55** ( $\text{EM}\odot 4\text{-MeC}_6\text{H}_4\text{OMe}$ ) $\cdot 4(4\text{-MeC}_6\text{H}_4\text{OMe})$  (crystallized from 4-MeC<sub>6</sub>H<sub>4</sub>OMe–PhNO<sub>2</sub>–EtOH, determined at 298 K),  $a = 16.864(6)$ ,  $b = 18.652(7)$ ,  $c = 16.034(6)$  Å,  $\alpha = 104.59(1)^\circ$ ,  $\beta = 117.93(1)^\circ$ ,  $\gamma = 101.76(1)^\circ$ ,  $V = 3995$  Å<sup>3</sup>,  $Z = 1$ , 10 977 unique reflections,  $5630 > 2\sigma(I)$ , maximum  $2\theta = 115^\circ$ ,  $\text{CuK}\alpha$  radiation, was refined to  $R = 0.16$ . No decay in standard reflections was observed (68.5 h). One molecule of 4-MeC<sub>6</sub>H<sub>4</sub>OMe is located in the host cavity. The 4-MeC<sub>6</sub>H<sub>4</sub>OMe extends into one bowl with Me 0.90 Å below the plane through the four bridge oxygens (plane **a**, see **56**). The six ring guest atoms have been constrained to be planar and the normals to this plane and the plane through the four oxygen atoms form an angle of 88°.

The crystal structure of **37** ( $\text{EE}\odot 4\text{-MeC}_6\text{H}_4\text{OMe}$ ) $\cdot 4(4\text{-MeC}_6\text{H}_4\text{OMe})$  (crystallized from 4-MeC<sub>6</sub>H<sub>4</sub>OMe–PhNO<sub>2</sub>–EtOH, determined at 298 K),  $a = 16.827(5)$  Å,  $b = 18.611(6)$  Å,  $c = 16.242(5)$  Å,  $\alpha = 104.08(1)^\circ$ ,  $\beta = 117.78(1)^\circ$ ,  $\gamma = 102.20(1)^\circ$ ,  $V = 4040$  Å<sup>3</sup>,  $Z = 1$ , 11 093 unique reflections,  $5865 > 2\sigma(I)$ , maximum  $2\theta = 115^\circ$ ,  $\text{CuK}\alpha$  radiation,

(8) (a) SHELX86 (**55**, **37**, and **52**); SHELXS-90 (**50**): Sheldrick, G. M. *Acta Crystallogr.* **1990**, *A46*, 467–473; (b) Sheldrick, G. M. SHELXL-93, **1996**, in preparation.

was refined to  $R = 0.13$ . An 18% decay in intensities of standard reflections was observed (69.1 h). One Me of the guest extends into one bowl with the C atom 0.90 Å below the plane through the four bridge oxygens (plane **a** of **56**). The six ring guest atoms have been constrained to be planar and the normals to this plane and the plane through the four oxygen atoms form an angle of 86°.

The crystal structure of **52** ( $\text{PE}\odot 4\text{-MeC}_6\text{H}_4\text{OMe}$ ) $\cdot 4\text{-MeC}_6\text{H}_4\text{OMe}$  (crystallized from 4-MeC<sub>6</sub>H<sub>4</sub>OMe–PhNO<sub>2</sub>–EtOH) was first attempted at 298 K:  $a = 15.723(10)$  Å,  $b = 17.544(11)$  Å,  $c = 14.800(9)$  Å,  $\alpha = 113.46(2)^\circ$ ,  $\beta = 94.81(2)^\circ$ ,  $\gamma = 94.91(2)^\circ$ ,  $V = 3700$  Å<sup>3</sup>,  $Z = 1$ . The structure was solved, but the differences in the two bowls of the host could not be resolved. Accordingly data were collected for the same crystal at 175 K:  $a = 15.488(11)$  Å,  $b = 17.349(5)$  Å,  $c = 14.550(6)$  Å,  $\alpha = 113.66(3)^\circ$ ,  $\beta = 93.74(5)^\circ$ ,  $\gamma = 95.30(4)^\circ$ ,  $V = 3543$  Å<sup>3</sup>,  $Z = 1$ , 10 538 unique reflections,  $6188 > 2\sigma(I)$ , maximum  $2\theta = 120^\circ$ ,  $\text{CuK}\alpha$  radiation, refined to  $R = 0.18$ . A 7% decay in intensities of standard reflections was observed (188.11 h). The six ring guest atoms have been constrained to be planar and the normals to this plane and the plane through the four oxygen atoms (plane **a** of **56**) form an angle of 96°. One Me of the guest penetrates the bowl of the host, with the C of Me 0.94 Å below plane **a**.

The crystal structure of **50** ( $\text{PE}\odot 1,2\text{-(MeO)}_2\text{C}_6\text{H}_4$ ) $\cdot 6(1,2\text{-(MeO)}_2\text{C}_6\text{H}_4)$  (crystallized from 1,2-(MeO)<sub>2</sub>C<sub>6</sub>H<sub>4</sub>–PhNO<sub>2</sub>–EtOH, determined at 175 K),  $a = 17.288(18)$  Å,  $b = 18.419(17)$  Å,  $c = 16.740(14)$  Å,  $\alpha = 91.25(8)^\circ$ ,  $\beta = 117.04(6)^\circ$ ,  $\gamma = 69.95(7)^\circ$ ,  $V = 4402$  Å<sup>3</sup>,  $Z = 1$ , 11 951 unique reflections,  $9238 > 2\sigma(I)$ , maximum  $2\theta = 120^\circ$ ,  $\text{CuK}\alpha$  radiation, was refined to  $R = 0.16$ . A 5% decay in intensities of standard reflections was observed (162.30 h). The angle between the normal to the least-squares plane of the benzene ring of the disordered guest and the normal to the plane of the four bridge oxygen atoms is 89°, and one of the OMe methyl carbons penetrates the bowl to 0.56 Å below plane **a**.

**Acknowledgment.** We warmly thank the U.S. Public Health Service for supporting grant GM-12640.

**Supporting Information Available:** Crystallographic data, atomic coordinates and displacement parameters, and bond lengths and bond angles for each of the four crystal structures have been deposited in electronic form. See any current masthead page for ordering information and Internet access instructions.

JA963379R